Palaeogeography, Palaeoclimatology, Palaeoecology 412 (2014) 223–240

Contents lists available at ScienceDirect

Palaeogeography, Palaeoclimatology, Palaeoecology

journal homepage: www.elsevier.com/locate/palaeo

Stratigraphy and palynology of a late Paleozoic glacial paleovalley in the Andean Precordillera, Argentina

Carlos O. Limarino [a,*], Pablo J. Alonso-Muruaga [a], Patricia L. Ciccioli [a], Valeria S. Perez Loinaze [b], Silvia N. Césari [b]

[a] IGEBA, Departamento de Geología, Facultad de Cs. Ex. y Nat., Universidad de Buenos Aires, Pabellón 2, Ciudad Universitaria, C1428EHA, Buenos Aires, Argentina
[b] Museo Argentino de Ciencias Naturales "B. Rivadavia", Av. Ángel Gallardo 470, C1405DJR, Buenos Aires, Argentina

ARTICLE INFO

Article history:
Received 3 April 2014
Received in revised form 21 July 2014
Accepted 28 July 2014
Available online 8 August 2014

Keywords:
Carboniferous
Glacial
Stratigraphy
Palynology
Argentina

ABSTRACT

A new locality where Carboniferous glacial diamictite appears confined to paleovalleys is described in the north of the Argentinian Precordillera. The glacial deposits of the lower part of the Carboniferous Quebrada Larga Formation are divided in three stratigraphic intervals, all of them confined to a paleovalley carved into the granitic and high-grade metamorphic basement. The lower section is composed of different types of massive and stratified diamictite interpreted to record reworking of previously deposited poorly sorted glacial sediments. The middle section comprises shale with dropstones, lenticular beds of diamictite and large-scale cross-bedded sets of sandstone and conglomerate. These rocks represent a more advanced stage of deglaciation that comprises the following succeeding steps: 1) amelioration of the climatic conditions, melting of glaciers, fluvial erosion, 2) the formation of a water body (onset of the fjord system) and 3) a later progradation of Gilbert-type deltas. Diamictite is missing in the upper section, which is chiefly formed by cross-bedded sandstone and conglomerate deposited in braided fluvial plains. A quantitative analysis of palynological assemblages through the sequence allowed a reconstruction of the dynamics of the vegetation developed during the filling of the paleovalley. The presence of monosaccate pollen grains supports an age not older than Serpukhovian and the recognition of the characteristic species of the *Raistrickia densa–Convolutispora muriornata* Biozone reinforces a late Serpukhovian–Bashkirian age for the assemblages.

1. Introduction

Upper Mississippian and Lower Pennsylvanian glacial and glacial influenced diamictites have been widely recognized in the Andean late Paleozoic basins from Argentina and Bolivia (González, 1981; Limarino and Gutiérrez, 1990; López Gamundí, 1997; López Gamundí et al., 1992; Limarino et al., 2002; González Bonorino, 1992; López Gamundí and Martínez, 2000; Perez Loinaze et al., 2010a,b, among others). Although the major part of the glacial deposits correspond to proximal and distal glaciomarine accumulations (López Gamundí, 1987, 1997; Perez Loinaze et al., 2010a), several papers have demonstrated the existence of coarse-grained successions sedimented in glacial paleovalleys interpreted as fjords (Milana and Bercowski, 1990; Kneller et al., 2004; Dykstra et al., 2006, 2007; Limarino et al., 2010).

The filling and stratigraphy of these glacially controlled paleovalleys can be divided, in broad terms, into two major sections. The lower one, resting on the floor of the paleovalleys, corresponds to complex successions of coarse-grained tillite, resedimented diamictite and shale containing ice-rafted debris (Marenssi et al., 2005; Dykstra et al., 2007). Striated pavements carved not only on the floors and walls of the paleovalleys but also on previously deposited glacial diamictite forming boulder striated pavements suggest recurrent expansion and retraction of glaciers (González, 1981; López Gamundí and Martínez, 2000; Marenssi et al., 2005; Alonso-Muruaga et al., 2011).

The upper section records an important postglacial marine transgression recognized in the whole of the Andean basins of Argentina (Limarino and Spalletti, 2006). This transgression flooded glacial paleovalleys forming thick successions of shale with dropstones, resedimented, fine-grained diamictite, mudstone and interestratified shale and fine-grained sandstone. The paleoenvironmental effect of the transgression was the nearly synchronous formation of fjord environments along the eastern margin of the Argentine Protoprecordillera (Marenssi et al., 2005; Limarino et al., 2006; Dykstra et al., 2007).

In the Argentine Precordillera, a good example of glacially influenced paleovalley occurs in the Cerro Veladero area, at the lower part of the Quebrada Larga Formation (Scalabrini Ortíz, 1973, Fig. 1). The existence of a glacial paleovalley and glacial influenced diamictite was largely ignored in the region probably due to the scarce studies focused on the Late Paleozoic stratigraphy. An exception was Scalabrini Ortíz and Arrondo (1973) who made a detailed study on the Late Paleozoic succession cropping out in the Veladero area. Unfortunately the section

* Corresponding author. Tel.: +54 11 45763329.
E-mail address: oscarlimarino@gmail.com (C.O. Limarino).

http://dx.doi.org/10.1016/j.palaeo.2014.07.030
0031-0182/

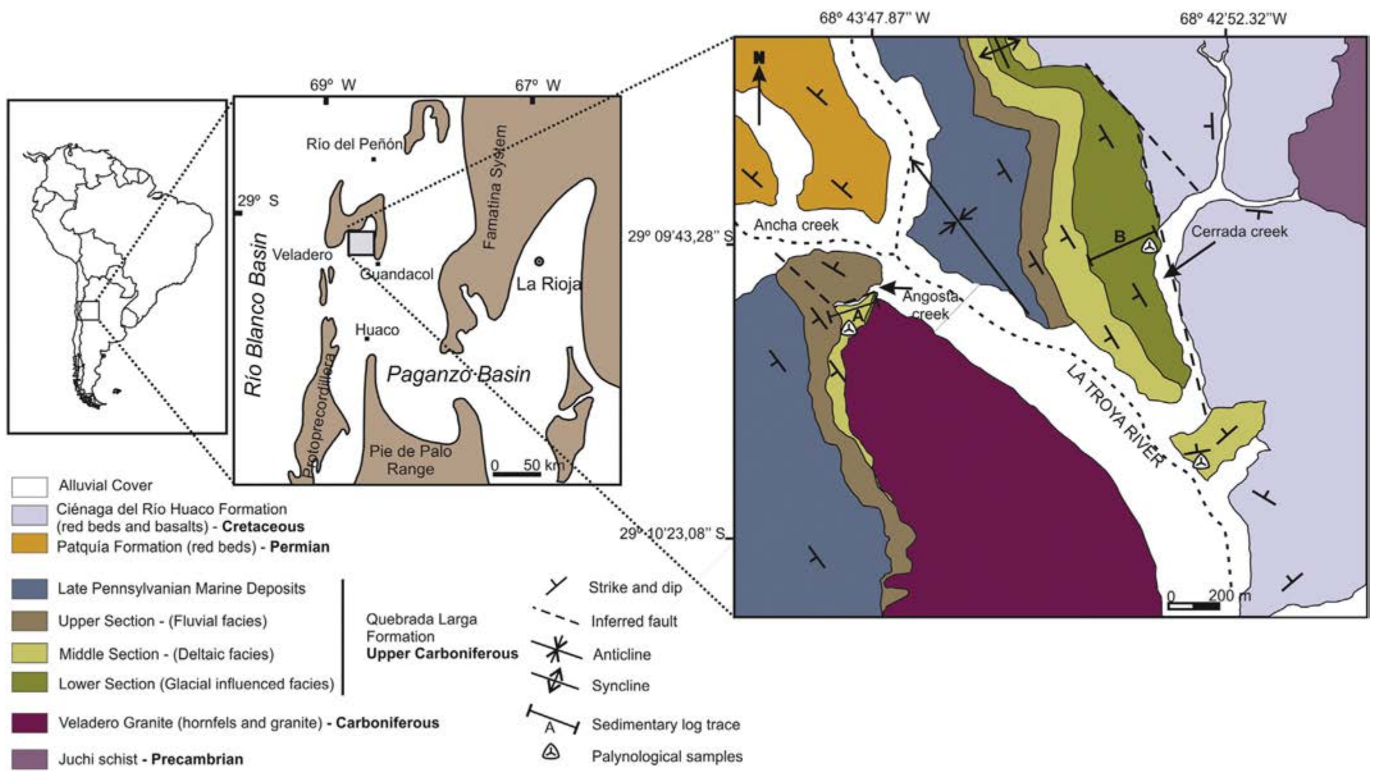

Fig. 1. Location and geologic map of the Cerro Veladero area. A and B indicate the position of the sedimentary sections shown in Fig. 4.

studied by Scalabrini OrtÍz and Arrondo (1973) is located to the south of the Cerro Veladero where neither the irregular topography of the paleovalley nor glacial diamictite appear.

At present, the biostratigraphy of Gondwanic glaciation in Late Carboniferous paleovalleys was carried out considering the glacial and glacial-related successions, as a whole, without separating the basal

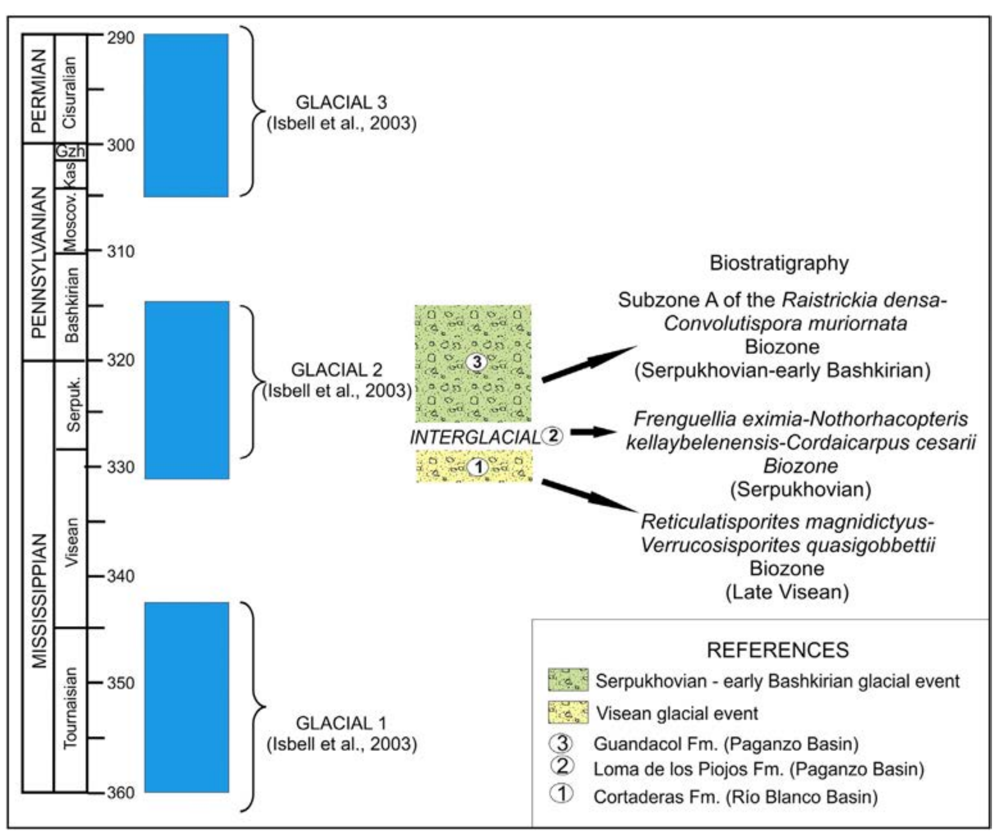

Fig. 2. Major glacial events recognized by López Gamundi (1989) and Isbell et al. (2003) during the Carboniferous and Early Permian. The studied strata belong to the glacial event 2 which can be divided in two different glacial episodes (1 and 3 in the figure) separated by an interglacial period (2 in the figure).

coarse-grained filling from the mainly fine-grained rocks deposited during postglacial transgression. However, at least two glacial events close to the Mississippian–Pennsylvanian boundary have been recognized in the western basins of Gondwana (Suárez-Soruco, 2000; Caputo et al., 2008; Perez Loinaze et al., 2010a, Fig. 2). The older one, probably Visean in age, seems to have a more restricted regional distribution while the younger, Serpukhovian–early Bashkirian, is widely recorded in the Andean Basins (González, 1981; López Gamundí, 1984, 1997; Limarino and Gutiérrez, 1990; López Gamundí et al., 1992; Kneller et al., 2004; Dykstra et al., 2006, 2007; Limarino et al., 2010).

The aim of this paper is to analyze the sedimentology of a glacially influenced Carboniferous paleovalley and present detailed palynological research in order to establish the position of the studied succession within the late Paleozoic glacial stratigraphy.

2. Geological setting

The Cerro Veladero area is located in the north of the Andean Precordillera (La Rioja province, Argentina) within the western domain of the late Paleozoic Paganzo Basin (Azcuy and Morelli, 1970; Salfity and Gorustovich, 1983, Fig. 1).

The local basement of the basin is composed of two types of rocks: Mesoproterozoic high-grade methamorphic rocks belonging to the Juchi Orthogneiss (Varela et al., 1996, 2003), which composes the Sierra de Umango (Fig. 1) and an early Carboniferous granitic body that forms the Cerro Veladero, a prominent hill reaching an altitude close to 2400 m.

The granitic rocks are covered by light gray to yellowish gray sandstone, diamictite, conglomerate, shale (in some cases carbonaceous shale) and scarce coal beds included in the Quebrada Larga Formation (up to 250 m thick, Fig. 3). The Quebrada Larga Formation (upper section of the Paganzo Group, Azcuy and Morelli, 1970) is divided in two informal members; the lower corresponds to the glacial deposits analyzed here and it is a lateral equivalent to the Guandacol Formation defined eastward of the basin (Fig. 3). The upper member includes fluvial conglomerate and sandstone covered by marine fine-grained sandstone and mudstone belonging to the Late Pennsylvanian transgression. This upper member is time-equivalent to the Tupe Formation in the Eastern Precordillera (Fig. 3).

The Quebrada Larga Formation is overlain by latest Carboniferous–early Permian red beds included in the Patquía Formation which forms the upper section of the Paganzo Group (Figs. 1 and 3). Depositional environments of the Patquía Formation are characterized by drastic changes in the paleoclimatic conditions when compared with those of the Quebrada Larga Formation. Glacial deposits have completely disappeared and semiarid to arid climates are suggested by the occurrence of eolian, ephemeral fluvial and playa lake deposits (Limarino and Spalletti, 1986; López Gamundí et al., 1992; Spalletti et al., 2010).

Finally, the younger rocks correspond to Cretaceous red beds and basalts belonging to the Ciénaga del Río Huaco Formation for which an age of 108.1 ± 4.4 Ma was obtained by Tedesco et al. (2007, Figs. 1 and 3).

3. Stratigraphy of late Paleozoic glacial events in western Gondwana

First considered as a nearly continuous glacial era, the Late Paleozoic Gondwanan glaciation is better understood as a long period in which glacial and non-glacial events alternated successively and diachronously throughout Gondwana. López Gamundí (1997) considered three major glacial episodes, which occurred during: 1) the latest Devonian–earliest Carboniferous, 2) middle Carboniferous and 3) late Carboniferous–Early Permian. Recently, Isbell et al. (2003) and Fielding et al. (2008) have considered different glacial intervals along Gondwana (Fig. 2).

For the western Gondwana basins, Perez Loinaze et al. (2010a) recognized two glacial periods within the Glacial 2 interval of Isbell et al. (2003), which were separated by an interglacial interval (Fig. 2). Recently, Limarino et al. (2014) identified the interglacial interval in the Loma de Los Piojos Formation, in which Balseiro et al. (2009) described remains of the early Serpukhovian *Frenguellia eximia–Nothorhacopteris kellaybelenensis–Cordaicarpus cesarii* Biozone that would indicate warm temperate conditions rather than glacial climates (Fig. 2).

Stratigraphically below plant-bearing horizons of the Loma de Los Piojos Formation glacial deposits occur, representing the first glacial period recognized in the Upper Member of the Cortaderas Formation

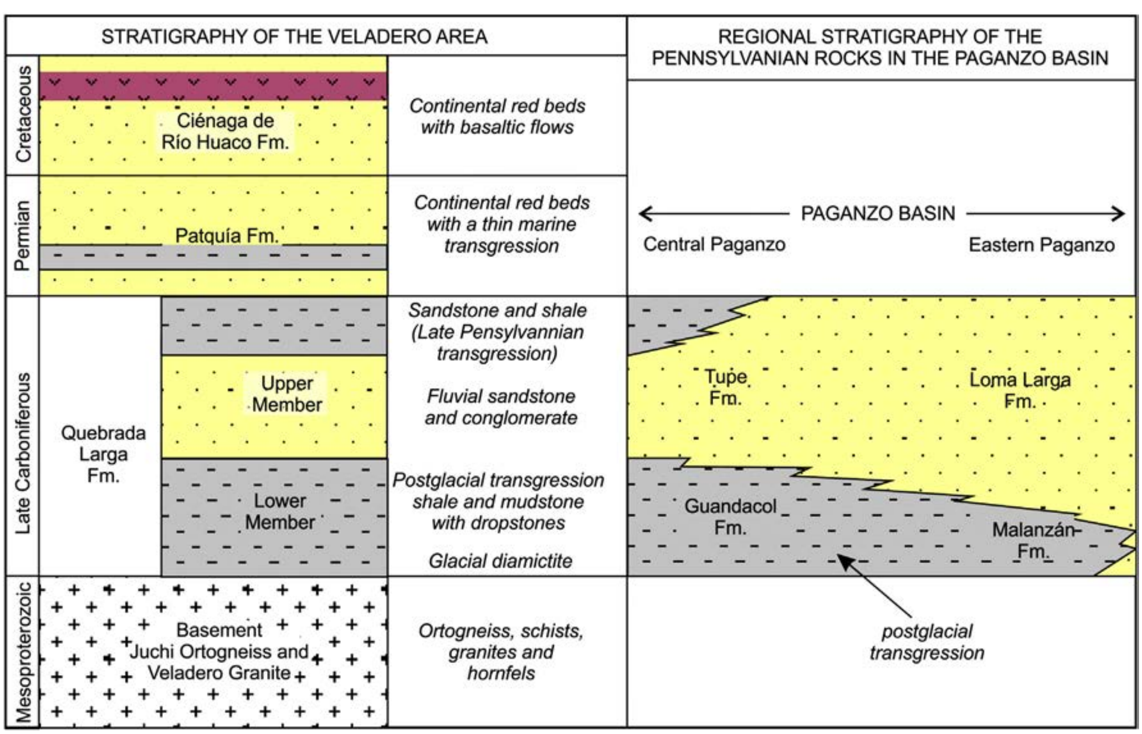

Fig. 3. Stratigraphic chart showing the regional correlations of the Carboniferous sequences in Paganzo Basin.

(Limarino and Césari, 1993; Perez Loinaze et al., 2010a, Fig. 2). This member comprises massive matrix-rich diamictite, massive clast-rich diamictite, stratified diamictite and shale with and without dropstones; all of them sedimented in a glaciomarine environment with a fluctuating sea level position (Perez Loinaze et al., 2010a). According to palynological data, the glacial event of the Cortaderas Formation is late Visean in age and consistent with radiometric ages presented by Gulbranson et al. (2010) for the Andesita Punta de Agua (335 ± 0.06 Ma), a lateral equivalent of Cortaderas Formation.

The existence of a Visean glaciation is not exclusive for the western late Paleozoic basins of Argentina since glacial successions of Visean age were reported from the Poti Formation (Amazonas Basin, Brazil), Faro Formation (Parnaíba Basin, Brazil) and Kaka Formation (Copacabana Basin, Bolivia) by Suárez-Soruco (2000), Melo and Loboziak (2003) and Caputo et al. (2008).

The next glacial event (second glaciation within the glacial 2 interval, Fig. 2) took place during the early Pennsylvanian (Serpukhovian–early Bashkirian). It is represented in the whole of the western Andean basins of southern South America. In the region considered in this paper, the Serpukovian glaciation is recorded in transitional environments identified in the lower part of the Guandacol, Agua Colorada and Malanzán formations (Paganzo Basin) as well as in the marine successions of the Hoyada Verde and Agua de Jagüel Formations (Calingasta-Uspallata Basin). The glacial interval is made up of massive diamictite (in part tillites), resedimented coarse- and fine-grained diamictite, shale with dropstones and dropstone-free shale (González, 1981; López Gamundí, 1984, 1997; Limarino and Gutiérrez, 1990; López Gamundí and Martínez, 2000; Limarino et al., 2002, 2010; Perez Loinaze et al., 2010a, b; among several others). Palynological remains obtained from these deposits were included in the *Raistrickia densa–Convolutispora murirnata* Biozone assigned to the Serpukhovian–early Bashkirian (=early Namurian by Césari and Gutiérrez, 2001). This age agrees with the age of the *Levipustula* fauna that characterizes this glacial interval in marine facies of the Hoyada Verde Formation (González, 1981; Taboada, 2010), and radiometric ages obtained by Gulbranson et al. (2010).

4. The Veladero glacial paleovalley: Sedimentology

Carboniferous glacial deposits in the Veladero area show an irregular distribution strongly controlled by the paleotopography carved into the basement rocks of the Juchi Orthogneiss and Veladero granite. The best glacial-paleovalley exposures are located in the northern slope of the Cerro Veladero (section A in Fig. 1 and A in Fig. 4) and along the Cerrada creek (section B in Fig. 1 and B in Fig. 4) where massive and resedimented diamictites are common. By contrast, the upper filling of the paleovalley is characterized by cross-bedded sandstone and conglomerate covered by fine-grained sandstone and shale very probably

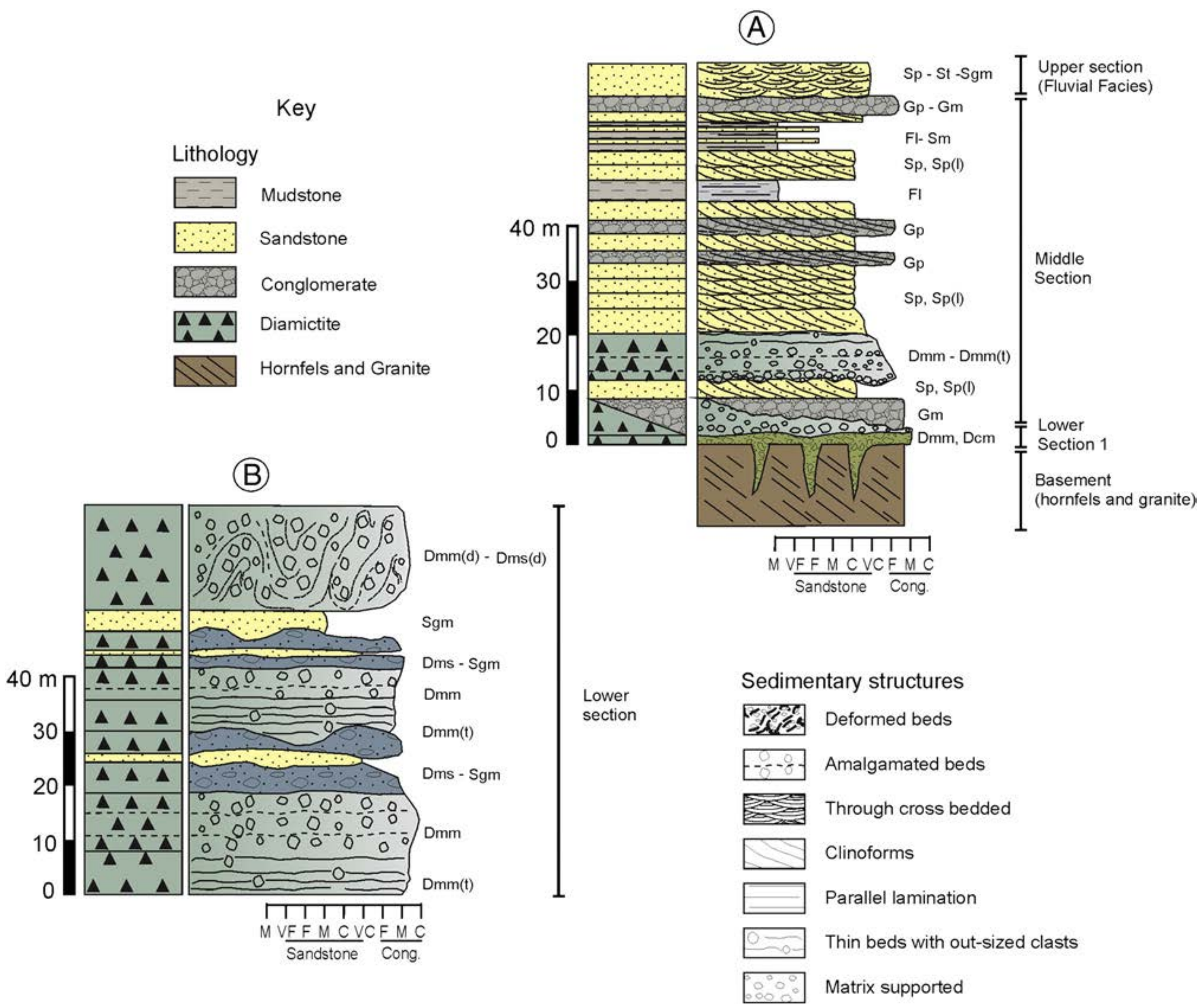

Fig. 4. Schematic stratigraphic sections of the Quebrada Larga Formation along the paleovalley, for location see Fig. 1.

representing fluvio-glacial and shallow marine postglacial deposits (B in Fig. 4).

The best view of the Carboniferous paleotopography is shown in the north flank of the Cerro Veladero, which formed the southern wall of the paleovalley (Fig. 5). Massive diamictite is dominant at the bottom of the paleovalley (Fig. 4 and point 1 in Fig. 5A), covered firstly by a thin interval of cross-bedded sandstone and conglomerate and then by fine-grained sandstone, dropstone-bearing shale, varve-like rhythmites, and large-scale sandstone and conglomerate forming Gilbert-type deltas (point 2 in Fig. 5A and B). Starting from point 3 in Fig. 5A shale are followed by cross-bedded medium- and coarse grained arkose and conglomerate overlying a slightly irregular topography. Finally at the top of the Veladero hill (point 4 in Fig. 5A and B) a new sequence of fine-grained sandstone and shale appears, but in this case shale with dropstones is missing. This fine-grained succession rest on the granite and represent the end of paleovalley filling and the loss of confinement. Taking into account the onlap of the Carboniferous succession, the strike and dip of the beds and correcting minor tectonic structures (small tectonic displacement) a minimum of 145 m in relief between the top and bottom of the paleovalley has been estimated.

The close relation of these deposits with glacial environments is suggested by the dominance of massive and stratified diamictite bearing faceted and striated clasts and the high proportion of dropstones, up to 120 cm in diameter, into the shale of the postglacial transgression deposits. Moreover, the presence of centimeter-scale diamictitic levels injected into the schist of the basement may suggest the presence of thin lodgment till deposits (lower section in Fig. 4A).

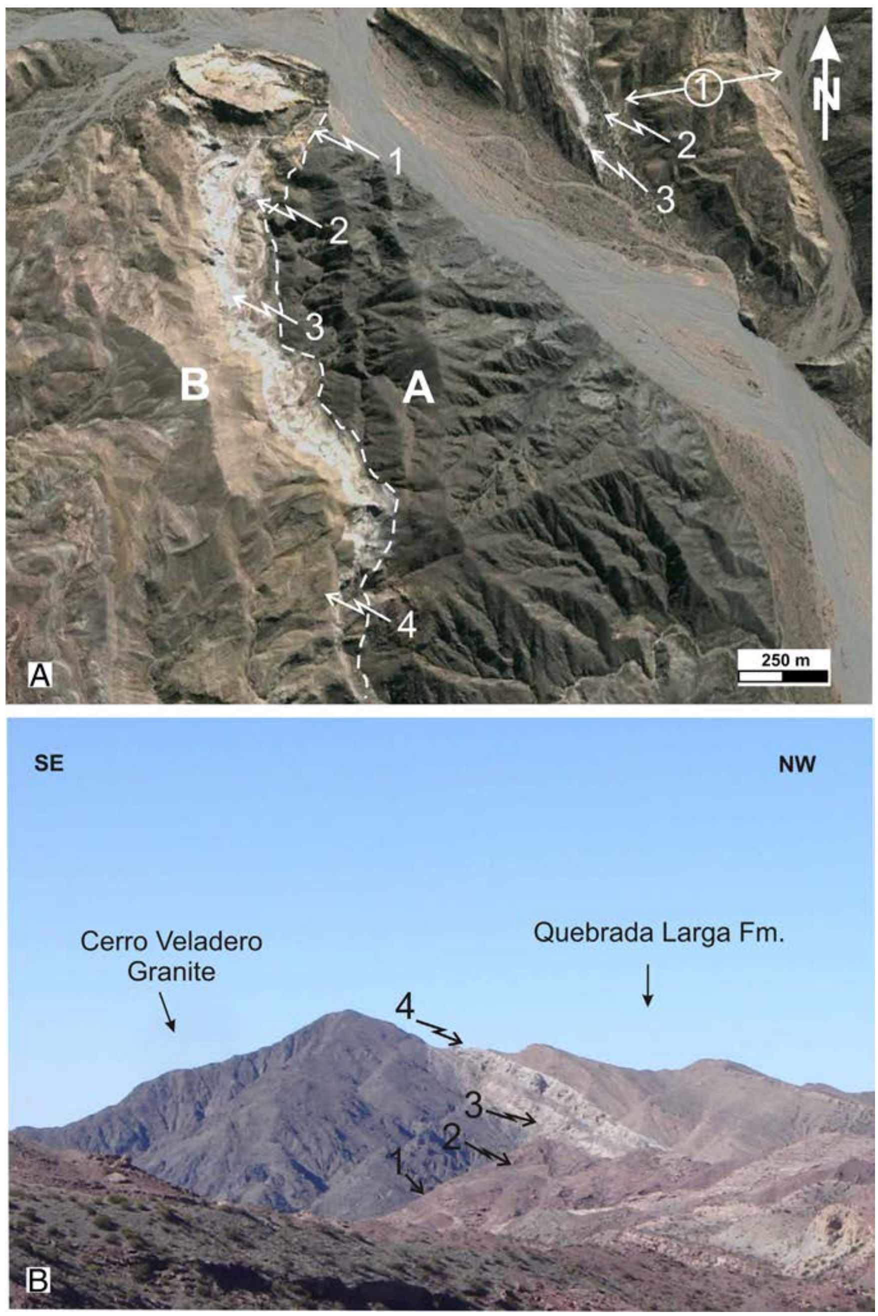

Fig. 5. A: Satellite image showing the southern wall of the paleovalley composed of granitic rocks belonging to the Veladero Granite (A in the photo) and Carboniferous rocks of the Quebrada Larga Formation (B) filling the incision. Note the onlap relation among Sections 1, 2 and 3 within the paleovalley (see also Fig. 1) which is finally overlain by marine deposits (Late Pensylvannian transgression) that form the top of the Quebrada Larga Formation (point 4). B: View of the outcrops towards the southern wall of the paleovalley.

The filling of the Veladero paleovalley has been divided in three stratigraphic intervals (Fig. 3, Table 1): 1. the lower section dominated by different types of diamictite, 2. the middle section composed of shale with dropstones, lenticular beds of diamictite and large-scale cross-bedded sandstone and conglomerate and 3. the upper section lacks diamictite and is characterized by cross-bedded sandstone and conglomerate together with thin mudstone and coal beds.

4.1. The lower section

4.1.1. Description

This section is composed of different types of massive and stratified diamictite, minor proportions of gravelly and coarse-grained sandstone and scarce mudstone and shale (Fig. 6). According to the paleogeography position into the paleovalley the thickness of the section ranges from 80 m to 2 m.

Diamictites comprise five different types (Table 1): 1. matrix-supported massive diamictite (Dmm), 2. interbedded stratified diamictite (Dms) and gravelly sandstone (SGm), 3. thinly bedded diamictite (Dmm(t)), 4. clast-rich monomictic diamictite (Dcm) and 5. deformed matrix-supported massive (Dmm(d)) or stratified diamictite (Dms(d)).

Matrix-supported massive diamictite occurs in irregular (or tabular?) stacked, commonly amalgamated, beds up to 2 m thick (Fig. 7A). Clasts (up to 100 cm) are subangular to rounded and in some cases exhibit faceted surfaces and glacial striations. Compositionally, clasts are dominated by granites, schists, quartz and green sandstone, floating in a fine-grained sandy (occasionally silty) matrix (Fig. 7B). Despite showing crude stratification in some cases (mainly diffuse coarse-tail-grading) we have included as massive all those diamictites that exhibit stratification over less than 10% of the unit thickness (Eyles et al., 1983).

Another quantitatively important type of diamictite corresponds to interbedded diamictite and pebbly sandstone beds ranging in thickness from a few decimeters to few meters. Diamictite is crudely stratified (Dms) and comprises matrix- and clast-supported paraconglomerate bearing clasts up to 12 cm in maximum diameter. Two different types of clast fabric have been identified; oriented long axes of clasts parallel to stratification and normal or more rarely reverse coarse-tail-grading. Clast composition is similar to the matrix-supported massive diamictite but the matrix is slightly coarser and dominated by fine-grained sand.

Gravelly sandstone is yellowish gray in color and form tabular massive beds, but in some cases a poorly defined normal grading has also been observed. Although the contact between diamictite and gravelly sandstone beds is usually sharp, in some cases a transition between both exists and the passage from the diamictite to the sandstone results in a progressive decrease in the number of larger clasts.

	Lithofacies	Interpretation
Upper Section	Sgm,Gp, Gm, Sr, St, Sp, Fm, Sm, Fl, C	Installation of fluvial systems
Middle Section	Gp, Gm, Sp, St Sp(l), Sm, Sr, Fm, Fl,Dms, Dmm(t), Dms(d)	Deglaciation and subsequent flooding of the palaeovalley (installation of the fjord system).
Lower Section	Dmm(t), Dmm, Dms Dmm(d),Dm(d), Dmm, Dcm,Sgm, Sm, Fm, Fl	Palaeovalley filling directly or indirectly influenced by glacial processes.

Fig. 6. Main characteristics and environmental interpretation of the three sections defined in the paleovalley fill.

Thinly bedded diamictite develops tabular centimeter-scale cycles (up to 9 cm thick) composed of fine-grained disorganized diamictite alternating with shale, mudstone or fine-grained sandstone. Diamictite bears clasts up to 5 cm in diameter, which float in a muddy matrix. Locally, the uppermost part of the beds shows thin sandy levels of ripple cross-lamination, indicating reworking of the diamicton by wave action or low-velocity currents. In almost all cases, diamictite beds are separated by thin laminae of mudstone and shale showing bedding plane bioturbation. Out-sized clasts (up to 30 cm in diameter) are common and show bending penetration as well as variable deformation, from slight to partial rupture of the lamination (Fig. 7C and D). The major part of out-sized clasts (dropstones) shows pentagonal shape, in some cases polished surfaces and less commonly striations in different directions.

Clast-rich and matrix-rich monomictic diamictite, bearing clasts up to 40 cm in diameter, have been only observed at the base of the glacial succession forming discontinuous, up to 1 m thick, beds resting on the contact with the basement. These beds fill the irregular topography carved into the basement and in some rare places thin levels of this lithofacies penetrate the basement rocks, suggesting injection (Figs. 4 and 7E), The distinctive characteristics of this type of diamictite are the high clast/matrix ratio (higher than 70), the monomictic composition of the clast (almost entirely formed by angular schist derived from the local basement, Fig. 7F) and its high induration.

The last type of diamictite corresponds to highly deformed matrix-supported stratified or massive diamictite, in some cases interbedded

Table 1
Lithofacies code and relative abundance in the three sections recognized in the glacial interval.

Lithofacies	Description	Lithofacies abundance		
		Lower S.	Middle S.	Upper S.
Dmm	Matrix-supported massive diamictite	Very common	Common	
Dmm(d)	Deformed matrix-supported massive diamictite	Common		
Dmm(t)	Thinly bedded matrix-supported massive diamictite	Very common	Very common/Sporadic	
Dms	Matrix-supported stratified diamictite	Very common	Common	
Dms(d)	Deformed matrix-supported stratified diamictite	Common	Sporadic	
Dcm	Clast-supported massive diamictite	Sporadic		
SGm	Gravelly sandstone	Very common	Common	Common
Gp	Cross-bedded conglomerate		Common	Very common
Gm	Massive conglomerate		Common	Very common
Sp	Cross-bedded sandstone		Common	Very common
Sp(l)	Large-scale cross-bedded sandstone		Common	
Sr	Ripple cross-laminated sandstone			Sporadic
Sh	Horizontally laminated sandstone		Sporadic	Common
Sm	Massive sandstone	Sporadic	Common	Common
Fm	Massive mudstone	Sporadic	Common	Sporadic
Fl	Shale	Sporadic	Very common	Sporadic
C	Coal			Sporadic

References: Very common (thick line) Common (thin line) Sporadic (dashed line) Very scarce or absent.

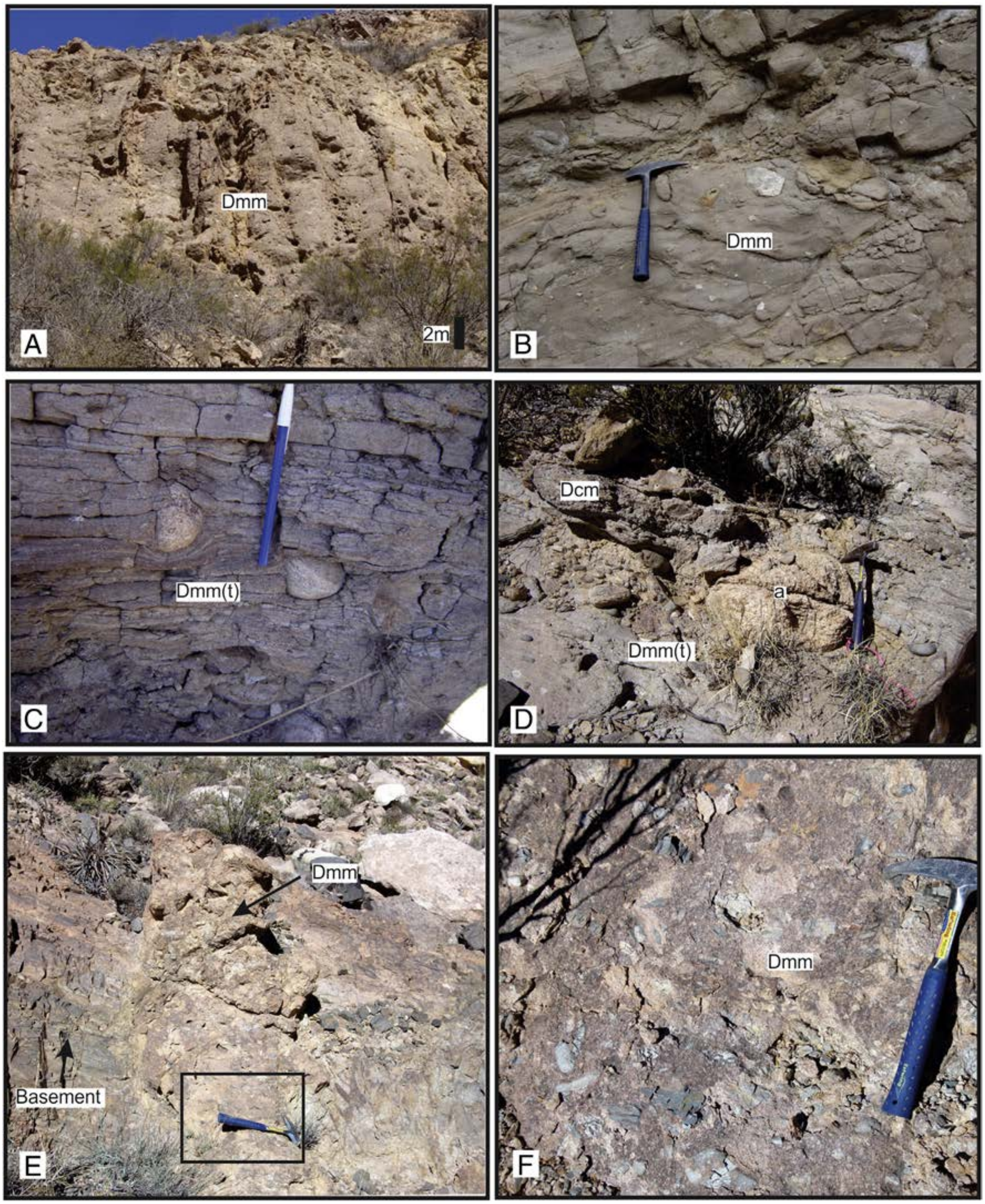

Fig. 7. A. aspect of the amalgamated beds of massive diamictite. B. Matrix-supported massive diamictite dominated by schist clasts indicating local provenance. C. Thinly-bedded massive diamictite showing out-sized clasts with impact structures (dropstones). D. Contact between clast-rich diamictite and thinly-bedded matrix-supported diamictite, note the presence of large granitic dropstones (a). E. Matrix-rich massive diamictite injected into basement rocks. F. Detail of E showing the monomictic composition of the clasts dominated by hornfels.

with gravelly sandstone. This diamictite occurs close to the contact between the lower and middle section and show intense sedimentary deformation including folds of decimetric to metric scale and small faults.

Interbedded between diamictite beds appear coarse- and medium-grained sandstone, mudstone and shale. Sandstone beds are irregular and lenticular in shape, generally thinner than 20 cm, showing internally massive or cross-stratified units in which dispersed gravelly clasts commonly occur. Shale and mudstone are dark gray, form tabular beds ranging in thickness from very thin millimeter-scale intercalations to 100 cm; within these fine-grained rocks it is very common the presence of randomly distributed large clasts interpreted as dropstones.

4.1.2. Interpretation

Several features suggest that the paleovalley fill was direct or indirectly influenced by glacial processes. For example, the existence of abundant out-sized clasts, interpreted in our case as dropstones, indicates rain-out from ice-rafted debris, and therefore deposition from icebergs. It is true that other mechanisms have been also proposed for dropstone deposition (Bennett et al., 1996; Doublet and Garcia, 2004) but the size, composition and abundance of the out-sized clasts found in the lower section rule out that they originated by biological rafting, flotation or formed by clast projection related to contemporary volcanism. In particular, the existence of polished surfaces and striations in some dropstones, together with the pentagonal shape observed in a great number of clasts, suggest iceberg derivation (Limarino and Gutiérrez, 1990).

The existence of graded structure, horizontal orientation of long axes of clasts and other types of crudely developed stratification indicate that the major part of the diamictite resulted from reworking of previously deposited poorly sorted glacial sediments ("flowtill" deposits of Hartshorn, 1958; Zielinski and van Loon, 1996).

Matrix-supported massive diamictite, showing absent or crude stratification, was probably deposited in proximal settings from debris flows in which, owing to the short distance of transport, size sorting was minimal (Eyles et al., 1983; Miall, 1985a). This type of debris flow commonly occurs in valleys during deglaciation when unconsolidated, and poorly sorted glacial sediments, rest on steep hillside from where they can be easily remobilized by seismic shacking or simply by collapse of unstable depositional slopes (Benn et al., 2005; Dallimore and Jmieff, 2010). An alternative interpretation, however, can be postulated by the clast-rich monomictic diamictite found at the contact with the basement rocks. These diamictite exhibits monomictic composition of clasts, lack of reworking, levels highly indurated and presence of probable injection into the basement rocks. Similar diamictite was described by Marenssi et al. (2005) in the Huaco area (100 km southwards) being considered as lodgement till deposits although in that case occur spatially related to striated pavements.

Interbedded diamictite and gravelly sandstone are interpreted as subaqueous debris flows and likely represent the alternation of clay-poor debris flows (De Blasio et al., 2006) and sandy debris flows (Shanmugam, 1996; Marr et al., 2001; Amy et al., 2005) or hyperconcentrated density flows of Mulder and Alexander (2001). Similarly, the major part of the cycles composed of thinly bedded diamictite alternating with fine-grained rocks (shale, mudstone and ripple cross-bedded fine-grained sandstone) record successive events of distal debris flows followed by settling from suspension, or low-velocity underflows, during calm periods. However, the marked rhythmicity in some of the thinner alternations of diamictite and shale could be due to debris rain-out, indicating periods of freezing and unfreezing of the water body.

Deformed diamictite, similar to those described herein, is relatively common at the top of diamictitic successions in the Paganzo basin prior to sedimentation of shale with dropstones belonging to the post-glacial transgression (Césari and Limarino, 2002; Marenssi et al., 2005; Dykstra et al., 2006; Alonso-Muruaga et al., 2011). Intense soft-sediment deformation is very common in paleovalleys and fjords during glacial retraction forming a wide scale of deformational structures from microscopic (galaxy structures, Van der Wateren, 1995; Huuse et al., 2012), to small slidings and also large folds and faults (Aber, 1982; Powell, 2005; Dykstra et al., 2007; Stoker et al., 2010).

In short, the major part of the lower section is interpreted as the result of different types of debris flow combined with release of clasts from icebergs, and in lesser extent, settling from suspension of fine-grained rocks and low-velocity underflows. The predominance of debris flow during deglaciation is probably the most prominent feature of the paraglacial environments. Debris flows would have been favoured by the high availability of debris accumulated in unstable slopes.

4.2. The middle section

4.2.1. Description

The middle section rests over an incision surface carved into the lower section, and its outcrops are confined to the paleovalley topography (Fig. 8). The relief of the incision surface is very irregular; in fact when the thicknesses of the lower section in the Angosta and Cerrada creeks are compared it is apparent that the relief of the incision surface is very high, taking into account that the major part of diamictite succession was eroded in the Angosta creek (Fig. 1). Commonly, the incision surface is covered by cross-bedded medium- to coarse-grained sandstone and polymictic conglomerate stratified in lenticular beds, and less commonly by transgressive shale or reworked diamictite.

Basically the middle section is composed of large-scale cross-bedded sandstone (Sp) and conglomerate (Gp), tabular beds of shale (Fl), interbedded sandstone (Sh,Sr) and mudstone (Fm) and lenticular beds of stratified diamictite (Dms, Dms(d)).

Cross-bedded sandstone and conglomerate commonly form clinoforms up to 2 m thick (Fig. 9A). Sandstone is gray and form lenticular beds (in some cases amalgamated), bounded by a lower erosive surface; decametric sets of both tabular and through cross-bedding are common as well as dispersed pebbles. Conglomerate is polymictic, clast-supported and show coarse- to medium-grained sandy matrix. Clasts are well rounded to subrounded, up to 15 cm in diameter, and formed by fragments of granites, quartz, schists, gneisses and green sandstone.

In many cases, conglomerate and sandstone form clinoforms interpreted as Gilbert-type delta deposits. The average dip angle of foresets varies from 12° to 20° showing a tangential decrease in steepness toward the foreset-bottomset contact. Foresets are composed of pebbly sandstone, coarse-grained sandstone and less commonly disorganized conglomerate, while the topset strata are dominantly made up by lenticular beds of cross-bedded or horizontal-bedded conglomerate and pebbly sandstone. The contact between topset and foreset beds is commonly erosive whereas gradual transitions are locally present. Finally, the bottomset accumulations correspond to fine-grained sandstone to siltstone showing massive or horizontal lamination, but locally toeset deposits of disorganized pebbly sandstone also occur.

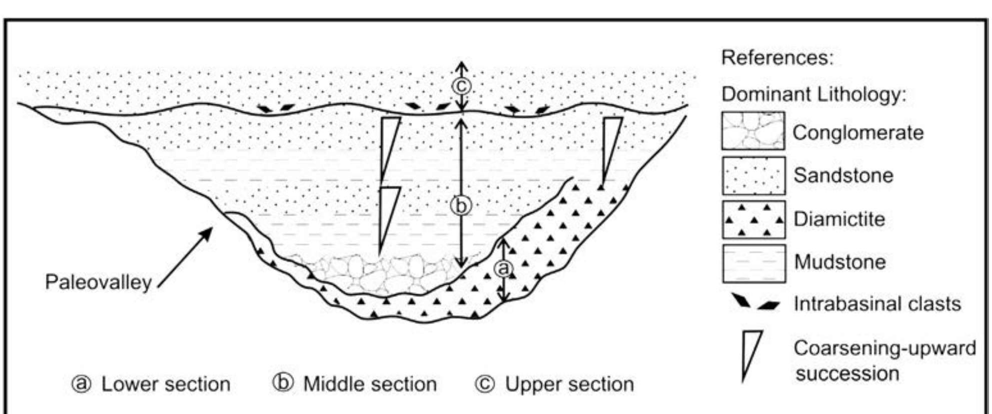

Fig. 8. Schematic representation of the paleovalley filling indicating the three defined section and bounding surfaces.

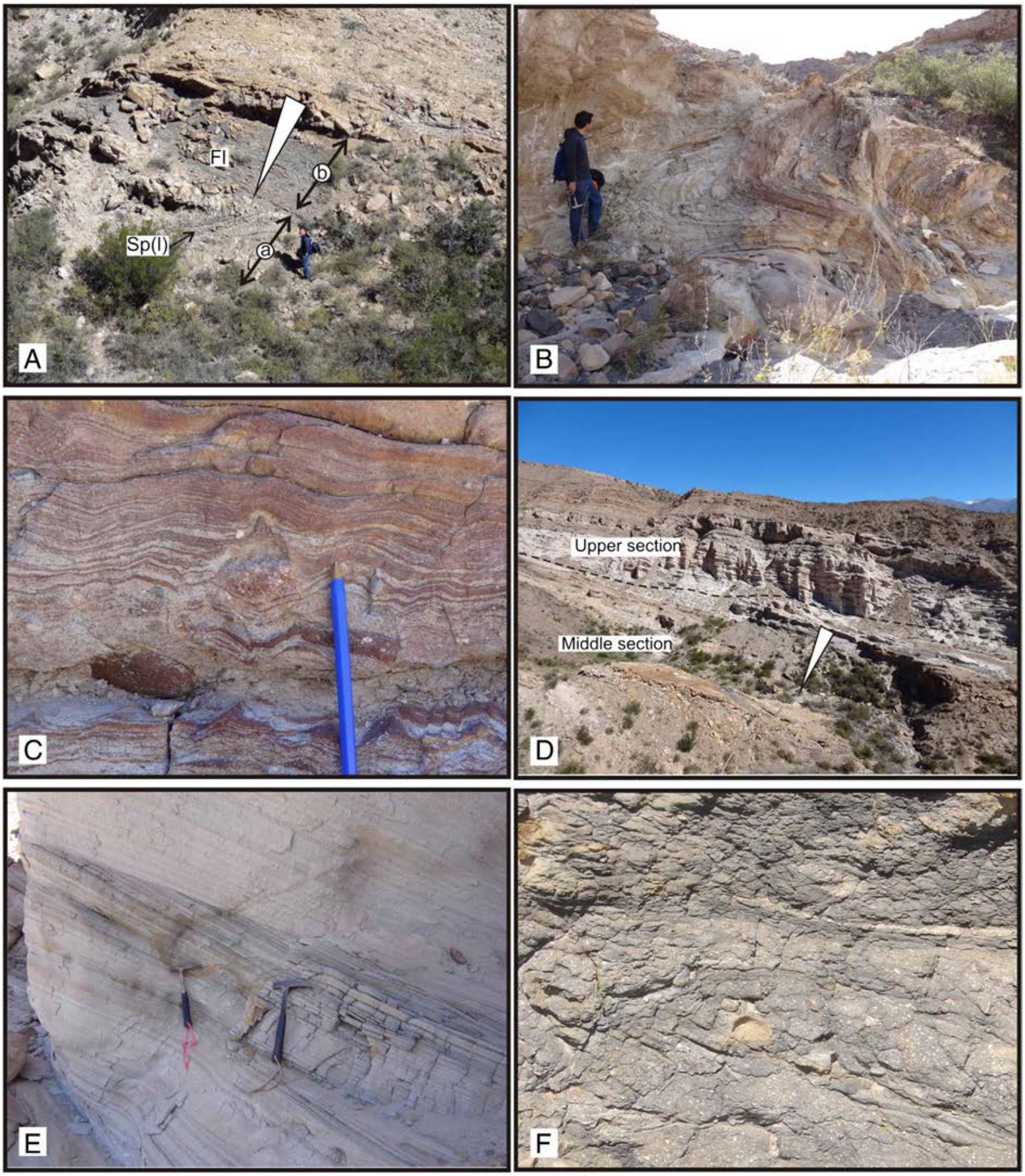

Fig. 9. A. Two different types of progradational cycles, metric-scale clinoforms (a) and abrupt transition from mudstone and shale to sandstone and conglomerate (b). B. Laminated sandstone and mudstone showing metric-scale synsedimentary folding. C. Rythmites containing out-sized clasts (dropstones). D. View of the contact between the middle and upper sections. E. Cross-bedded sandstone of the lithofacies Sp, which characterize the upper section. F. Carbonaceous mudstone that yielded palynological assemblages from the middle section.

In other cases, metric-scale coarsening-upward successions (up to 25 m thick), formed by fine-grained rocks at the base and sandstone or conglomerate at the top occur. These sequences do not exhibit inclined foresets and the existence of highly progradational deltas is deduced from the rapid transition from mudstone and shale (at the bottom) to cross-bedded sandstone and conglomerate (at the top) of the sequences (Fig. 9A). In some cases, the fine-grained rocks (shale and mudstone) forming the lower part of the coarsening-upward sequences bear plant remains belonging to the Pennsylvanian *Nothorhacopteris–Botrychiopsis–Ginkgophyllum* (NBG) Biozone (Archangelsky et al., 1987).

Metric scale interbedded sandstone and mudstone form successions up to 5 m thick below the clinoforms of the Gilbert deltas. Sandstones are medium- to fine-grained, green and gray in color; form tabular beds (up to 30 cm thick) showing massive bedding, cross-laminated beds and less commonly heterolithic lamination. Stratified mudstone occurs in tabular beds up to 20 cm thick, are mainly massive and rarely laminated. The contact between sandstone and mudstone beds is sharp and in some cases marked by load casts. Locally, laminated sandstone and mudstone exhibit synsedimentary deformation including small faults and metric-scale folds (Fig. 9B).

Fine-grained rocks are commonly found in this section and form tabular successions comprising shale, rhythmites and massive mudstone, all of which include out-sized clasts interpreted as dropstones (Fig. 9C). Shale is organic rich, dark gray to black and show delicate lamination. Rhythmites consist of interlaminated very fine-grained sandstone and siltstone (in some cases claystones). The sandy layer is massive or rarely exhibits current ripple-cross lamination, while siltstones are massive or in some cases crudely laminated. Massive mudstone is stratified in tabular beds ranging from a few centimeters to 20 cm thick and poorly preserved plant fragments have been identified in some levels.

Matrix-supported stratified diamictite appears randomly dispersed within the succession, either intercalated in the fine-grained rock intervals or associated with interbedded sandstone and mudstone successions. Diamictite, bearing clasts up to 10 cm, forms lenticular beds (up to 40 cm) with an erosive lower surface and crude stratification marked by diffuse coarse-tail-grading. In other cases diamictite is massive and forms tabular beds bounded by a sharp, but non erosive, lower surface.

4.2.2. Interpretation

When compared with the lower section, the middle section seems to represent a more advanced stage of deglaciation characterized firstly by fluvial erosion (incision surface), later fluvial sedimentation (cross-bedded sandstone and conglomerate) and then by the formation of a water body indicating the flooding of the paleovalley (fjord system). The lesser glacial influence is indicated by the lack of massive diamictite that could be interpreted as tillite, the abundance of fine-grained rocks and the presence of well-developed Gilbert-type deltas.

Cross-bedded conglomerate and sandstone, directly disposed over the erosive surface that separate Sections 1 and 2 (Fig. 8), are interpreted as fluvial deposits confined to the paleovalley, probably resulting from sediment reworking during glacial retraction.

Fine-grained rocks that commonly form the lower part of deltaic successions in the coarsening-upward cycles could result from different processes. In the case of finely laminated and frequently organic-rich shale they were likely settling from suspension and probably represent sedimentation in the deepest part of the water body where the supply of sand-size particles was low. In contrast, rhythmites would have resulted from alternating underflow and overflow currents. The coarser term of the rhythmites that comprises fine- and very fine-grained sand was transported into the basin by density-driven, low-velocity, underflow currents. The origin of the finer-grained term is more complex because silt, and even clay, could be carried either by very dilute underflows or settling from suspension out of meltwater plumes (Gustavson et al., 1975; Mustard and Donaldson, 1987; Cowan et al., 1999; Henry et al., 2010).

Although underflows can be generated in several subaqueous environments, their abundance in glacial and paraglacial valleys is undeniable. This is probably linked to several factors; the high amount of fine-grained sediments produced by glacial erosion, differences in temperature between melt water and the water body, the sudden supply of sediments during negative balance of the glaciers and the existence of steep slopes, not only on the hillsides, but also into the water body (e.g. delta fronts in Gilbert deltas; Gustavson et al., 1975; Limarino and Césari, 1988; Cowan et al., 1999; Dykstra et al., 2007).

The metric-scale coarsening-upward cycles, composed of shale at the base and conglomerate and sandstone at the top, indicate progradation of highly constructive deltas, some of which have preserved inclined foresets suggesting the presence of Gilbert-type deltas. Topset deposits formed by cross-bedded conglomerate and gravelly sandstone were likely deposited as gravelly bars in distributary fluvial channels on the deltaic platform. The predominance of erosive contacts between topset and foreset beds, as well as the lack of stacked Gilbert deltaic successions, suggests repetitive fluctuations of the relative base level.

The presence of cross-laminated (locally heterolithic) fine- to medium-grained sandstone interbedded with mudstone beds in the bottomset interval are interpreted as distal mouth bar accumulations (Schomacker et al., 2010). Sporadically, these deposits pass into disorganized conglomerate and gravelly sandstone at some foreset toes, documenting gravity flows that reworked coarse material from platform and delta front locations.

The whole of the diamictite of the middle section is stratified and therefore results from gravity flows into the water body. In the case of diamictite stratified in lenticular beds, showing clasts up to 10 cm and diffuse coarse-tail grading probably were feeder channels of the thinly stratified tabular diamictite without erosive base.

It is worth noting that along the major part of the middle section dropstones occur, which indicate that glaciers were in contact with the water body during the major part of sedimentation of the middle section. Indeed, the dropstones can appear isolated or concentrated forming irregular levels, in this last case grounded iceberg on the fjord bottom could have formed iceberg dump till deposits as described by Thomas and Connell (1985).

4.3. The upper section

4.3.1. Description

The upper section is different from the two previously described because of the lack of diamictite, dropstones, synsedimentary deformational structures, and the very scarce abundance of fine-grained rocks. Basically, the upper section is almost entirely composed of cross-bedded coarse-grained sandstone and conglomerate, which rest on a low-relief incision surface carved into the middle section beds (Figs. 8 and 9D).

The upper section is widely dominated by lenticular stacked beds of white or whitish gray coarse-grained sandstone and granule conglomerate which can be divided into cross-bedded (Sp, Gp), horizontal-bedded (Sh, or low-angle cross-bedded) and massive (Sm, Gm) facies. Cross-bedded sandstone and granule conglomerate are the most abundant; they form lenticular beds, up to 40 cm thick, bounded by erosive lower surfaces over which intrabasinal clasts of mudstone locally appear. The major part of cross-bedded sets is medium- to large-scale and form tabular or trough geometries. Slightly erosive downstream inclined surfaces (third-order DA bounding surfaces of Miall, 1985b, 1996) are common.

Horizontal-laminated and low-angle cross-bedded sandstone and granule conglomerate appear stratified in more continuous and thinner beds than the cross-bedded sandstone above described; in these cases the lower surface of the beds is plane or slightly erosive. Finally, massive sandstone and granule conglomerate appear randomly along the succession.

Conglomerate, bearing clasts larger than 50 mm, form about 30% of the section; they correspond to clast-supported orthoconglomerate stratified in lenticular beds with well-developed erosive surfaces. Clasts are well rounded and composed of quartz, gnesises, migmatite, medium-grained schist, green sandstone and scarce K-feldspar. Conglomerate exhibits large-scale cross-stratification or form massive beds. Low-angle cross-stratification can be identified in rare cases.

The uppermost part of the upper section shows a strong compositional change since coarse-grained sandstone and conglomerate are replaced by fine-grained sandstone, thin levels of organic-rich mudstone and thin coal beds. Fine-grained sandstone show horizontal lamination frequently associated with parting lineation, ripple cross-lamination and ripples at the top of the beds. Locally ripple cross-lamination is composed of alternated layers of sand and mud forming heterolithic structures.

Mudstone, dark gray in color, is stratified in massive and less frequently laminated beds bearing plant remains in variable degree of preservation. Lastly, at least two levels of laterally discontinuous coals plenty of plant remains have been identified intercalated between fine grained-sandstone.

The top of this section is marked by an important incision surface which, in turn, is covered by a thick succession of cross-bedded conglomerate and coarse-grained sandstone.

4.3.2. Interpretation

The upper section is genetically very different from the two previously considered, since reworked diamictite linked to paraglacial environments and fine-grained rocks deposited during the postglacial transgression are missing. The lower and middle parts of this section were deposited by fluvial systems that showed marked channel instability and very scarce lateral migration; the lenticular form of beds suggests frequent channel avulsion and the presence of third-order DA surfaces (down-stream accretion surfaces, Miall, 1985b) indicates downstream migration of bars rather than lateral migration.

The wide dominance of conglomerate and coarse-grained sandstone, the lenticular form of beds with erosive bounding surfaces and the lack of fine-grained sediments lead us to assume that braided fluvial systems formed the major part of the middle section. Disorganized granule conglomerate, immediately above the lower erosive base, seems to be deposited as channel lag accumulations or small core bars. According to geometry and thickness of the cross-bedded sets two major types of bars are recognized. Firstly, those formed by large to medium scale cross-bedded sets showing moderate to high dip angles of foresets, which are ascribed to transverse bars of moderate relief. Secondly, the major part of low-angle cross-bedded sandstone which could represent low-relief longitudinal or transversal bars.

Finally, the fine-grained sandstone, mudstone and coal beds, identified at the top of the section, form a key level along the Paganzo Basin which seems to be related to a short-time sea-level rise that only flooded the western area of the basin (Desjardins et al., 2009; Tedesco et al., 2010). This transgression established paralic conditions in the coastal region and increased the accommodation space in alluvial plains, favoring the formation not only of organic-rich mudstone but also coal beds with plenty of plant remains in different parts of the basin.

5. The Veladero glacial paleovalley: palynology

Palynologycal studies in the three sections of the paleovalley infill were performed in order to: 1. establish the age of the deposits, 2. determine if measurable differences exist in the age of the sections filling the palaeovalley, or on the contrary, if the paleovalley was quickly filled, and 3. analyze if significant differences exist in the recovered palynofloras, and consequently in the nature of the paleovalley vegetation, within and between the analyzed sections.

Twenty productive palynological samples were recovered in the studied deposits; all the samples are located at the Museo Argentino de Ciencias Naturales "B. Rivadavia," Palynological Collection (BA Pal). All the sections yielded biostratigraphically significant species that allow assessing the age of the whole valley infill.

5.1. The lower section

This assemblage shows a well-balanced ratio between pollen and spores moderately well preserved (Fig. 10). Similar proportions were identified in some samples from glacilacustrine deposits of the coeval Guandacol Formation (Perez Loinaze and Césari, 2012). The representative and significant palynomorphs found in the basal diamictite are the monosaccate pollen grains. The sample is characterized by the presence of *Potonieisporites brasiliensis*, *Potonieisporites densus*, *Plicatipollenites malabarensis*, *Plicatipollenites trigonalis*, *Caheniasaccites ovatus* and *Cannanoropollis janakii*. Spores are abundantly represented (56%) by smooth and ornamented specimens including *Raistrickia densa*, *Raistrickia rotunda*, *Convolutispora muriornata*, *Cyclogranisporites firmus*, *Grossusporites microganulatus*, *Reticulatisporites passaspectus, Tricidarisporites gutii* (Figs. 11.12) and *Cristatisporites* spp. The diversity is relatively high in this unique sample with 41 species (Fig. 12). Tetrads of *Lundbladispora*, ornamented and zonate spores indicate the local vegetation of moist sites surrounding the depositional environment. The scarce presence of *Tetraporina punctata* and *Portalites gondwanensis* is indicative of fresh-water (Lindgren, 1980; Zippi, 1998), although some authors suggested a brackish environment for these algae palynomorphs (Cazzulo-Klepzig et al., 1995).

This palynological assemblage is generically referable to the *Raistrickia densa–Convolutispora muriornata* (DM) Biozone. The DM Biozone has been considered essentially late Carboniferous in northwestern Argentina (Césari and Gutiérrez, 2001; Césari et al., 2011). The absence of bisaccate taeniate pollen grains suggests its inclusion in the A Subzone of the DM Biozone. Therefore, this glacial interval can be referred with confidence to the younger glacial event recognized in the region (Fig. 2). Palynological assemblages of the older glacial event are clearly distinguished by the absence of pollen (Perez Loinaze et al., 2010a).

5.2. The middle section

The middle section was comprehensively sampled for palynology. Three sets of samples were analyzed. The first was taken from the carbonaceous mudstone deposited in prodelta settings; the second set comprises carbonaceous mudstone forming part of the mouth bars deposits of the delta-front subenvironment and the third set corresponds to carbonaceous shale belonging to interdistributary bays of the subaqueous deltaic platform (Fig. 10). Although secondary redistribution of palynomorphs by different types of currents produces similar assemblages in the fjord system, some differences among the assemblages can be recognized.

All samples contain well-preserved spores, whereas the larger saccate pollen grains are commonly in a fragmentary condition and usually are just recognized by the presence of their sacs. This condition prevents the taxonomic identification of most of the specimens, but this does not distort the diversity values because their participation is low in the section. The preservation of pollen grains suggests a transport from the upland surrounding areas or reworking by erosion of the fine-grained sediments of the incised underlying lower section.

The assemblages from the prodelta environment consist almost exclusively of terrestrial components. Despite its more distal position, the assemblages reach the higher diversity with 58 species. Spores dominate the assemblages (70–88%) and the vast majority (up to 67%) is ornamented. Less than 10% of the spore assemblage is assigned to *Lundbladispora*, a dispersed spore of lycopsids, but zonate spores of this group of plants, like *Vallatisporites* and *Cristatisporites*, are locally abundant. The monosaccate pollen grains range between 11% and 27%. Scarce specimens of the marine palynomorph *Navifusa* (Combaz et al., 1967; Tiwari et al., 1995), are recorded in only two samples together with *Tetraporina punctata* and *Portalites gondwanensis*, which could be indicative of a marine transitional environment.

Palynological assemblages from the delta-front show dominance of woody debris. Batten (1996) considered this abundance of comminuted wood typical of inner shelf deposits. Only one sample from this interval contains palynomorphs. The average portion of spores is about (95%). *Lundbladispora* occurs rarely but smooth spores increase markedly. Diversity of the spore assemblage is obviously low with 15 species.

The assemblages from the subaqueous deltaic platform are dominated by spores. The proportion of spores (96 %) is similar to the latter sample. The assemblages from this section are moderately diverse containing, overall, about 48 species. Frequency of *Lundbladispora* in some samples is almost as high as the number of ornamented species, reaching 47% to 71% of the spores. Probably, these samples where *Lundbladispora* is represented by numerous tetrads (indicative of little transport) are related to the local vegetation. It is clearly a replacement in the representation of lycopod spores, with a low participation of zonate spores. In the samples where *Lundbladispora* is in low proportion or absent there is an increase in smooth or ornamented spores (Fig. 10). The diagnostic species *Convolutispora* and *Raistrickia* (fern-related) reach more than the 10% in those samples with low representation of *Lundbladispora* spores. Rare specimens of monosaccate taeniate pollen

Stratigraphic interval	Sample (BAPal)	% *Lundbladispora*	% Ornamented	% Zonate	% Smooth	% *Convolutispora/ Raistrickia*	% Spores	% Pollen	% Algae	Environment
Upper Section	6447	0.0	29,0	5.9	50.0	0.3	85.2	14.8	0.0	Fluvial
	6446	0.3	45,0	0.9	31.3	11.8	89.6	10.2	0.2	
	6445	0.0	45.2	0.31	51.1	0.0	96.6	3.4	0.0	
	644	0.0	33.4	0.6	59.8	0,0	93.8	6.2	0.0	
Middle Section	6443	0.0	20.3	0.0	76.9	0.0	97.2	2.8	0.0	Deltaic platform
	6442	71.4	26.0	0.0	0.7	0.0	98.1	0.3	1.6	
	6441	51.1	46.3	0.0	1.6	0.0	99.0	1.0	0.0	
	6440	2.5	91.2	2.2	2.3	0.0	98.2	1.8	0.0	
	6439	15.3	65.9	1.9	7.3	1.0	91.4	8.6	0.0	
	6438	47.4	23.9	5.9	17.5	2.9	97.6	1.5	0.9	
	6437	4.0	56.0	8.0	14.0	11.0	93.0	7.0	0.0	
	6436	64.6	16.5	4.0	9.4	2.4	96.9	0.0	3.1	
	6435	0.0	9.0	0.0	71.0	19.0	99,0	1.0	0.0	
	6434	0.0	23.6	2.7	66.2	0.0	92.5	7.5	0.0	
	6433	0.8	15.3	35.7	40.1	4.4	96.3	3.7	0.00	Delta-front
	6432	9.7	14.2	29.8	10.0	8.0	71.7	27.3	1.0	Prodelta
	6431	2.5	33.5	9.5	17.4	12.7	75.6	23.7	0.7	
	6430	1.3	67.2	3.8	13.5	2.2	88.0	11.7	0.3	
	6429	6.5	14.0	42.3	3.6	3.6	70.0	30.0	0.0	
Lower Section	6428	0.0	27.6	5.7	17.9	4.8	56.0	44.0	0.0	Diamictites

Fig. 10. Relative abundance of spores and pollen grains in the different facies associations.

were identified in only one sample (Fig. 12-23). These specimens referred to *Striomonosaccites* sp. are very similar to those described by Ottone and Azcuy (1989) for coeval deposits of the Guandacol Formation at La Delfina Mine in the San Juan Province.

Macrofloral remains of the *Nothorhacopteris–Botrychiopsis–Ginkgophyllum* Biozone were recovered from these deposits of the deltaic platform.

A slight decrease of spores from coastal clastic facies to distal settings is observed. While the relative proportion of spores in the prodelta decreases in more than 20% of that of the deltaic platform, the input of pollen increases in the same proportion. Diversity is also increased from proximal to distal environments. Diversity at the prodelta is more than 15% of that observed in the coastal clastic facies.

The occurrence in the middle section of *Raistrickia densa*, *Raistrickia rotunda*, *Convolutispora muriornata*, *Ahrensisporites cristatus*, *Potonieisporites* spp. and *Plicatipollenites* spp. suggests the presence of the DM Biozone in this stratigraphic interval. The absence of *Protohaploxypinus* or bisaccate taeniate pollen, species that characterize the Subzone B, probably is indicative of the Subzone A.

5.3. The upper section

The assemblages of the lower part of the section differ from the other sections, although they are also dominated by spores constituting up to 96% of the total. The major difference is seen in the composition of the spore assemblage with a predominance of specimens with little or no ornamentation (30–59%), probably related to sphenopsids, ferns and pteridosperms. *Lundbladispora* and zonate spores are rare and the overall diversity remains moderately high with 29 species. Only one sample preserves *Tetraporina* specimens (Fig. 12-27). The recognition of *Raistrickia densa* and *Convolutispora muriornata* allows us to infer in this section the presence of the DM Biozone. In the same way, the lack of *Protohaploxypinus* pollen or other bisaccate taeniate, like *Striatoabieites*, prevents the recognition of the B Subzone. However, it should be noted that participation of pollen taeniate in assemblages referred to the B Subzone (late Bashkirian in age) is always lower than 2% (Césari et al., 2013).

6. Discussion and conclusions

One of the major issues in the stratigraphy of the glacial deposits in western Gondwana is to achieve biostratigraphical and sedimentological information that distinguishes the glacial accumulations formed during the Visean from those deposited during the Serpukhovian–early Bashkirian (Fig. 2).

Palynological assemblages recovered from the glacial-related deposits from the Quebrada Larga Formation are very useful to constrain their age. The presence of monosaccate pollen in the palynofloras supports an age not older than Serpukhovian according to the first worldwide records of these palynomorphs (Brugman et al., 1985; Loboziak and Clayton, 1988; Clayton et al., 1990; Zhu, 1993; Clayton, 1995). Moreover, the recognition of the characteristic species of the *Raistrickia densa–Convolutispora muriornata* Biozone reinforces a late Serpukhovian–Bashkirian age for the assemblages. Palynofloras related to glacial conditions and characterized by the presence of pollen have been reported from the Guandacol Formation, lower section of the Agua Colorada, Malanzán, Jejenes and Lagares formations from central–western of Argentina. None of these units contain bisaccate taeniate pollen grains and were referred to the A Subzone of the DM Biozone (Césari and Gutiérrez, 2001; Perez Loinaze et al., 2010a). Recent

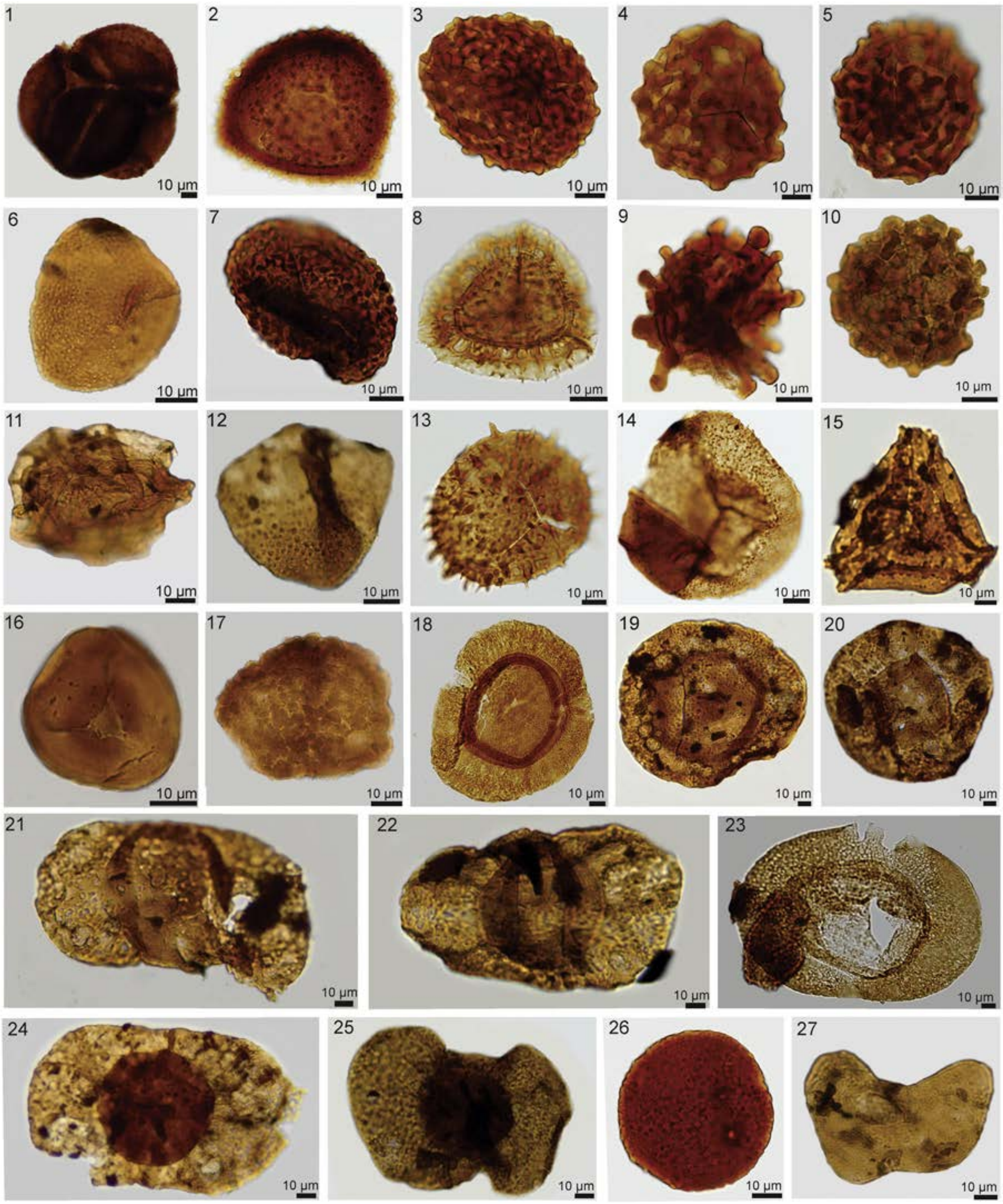

Fig. 11. 1. *Lundbladispora braziliensis* tetrad, 6438(1), D50; 2. *Lundbladispora braziliensis*, BAPal 6438(2), D 27; 3–5. *Convolutispora muriornata* BAPal 6438(2), W33/3; BAPal 6438(1) D56/3; BAPal 6438(2), B31; 6. *Microreticulatisporites punctatus*, BAPal 6442(2), S42/1, 7. *Verrucosisporites andersonii* BAPal 6436(1), F27/4, 8. *Vallatisporites* BAPal 6438(1), L32/3, 9. *Raistrickia densa* BAPal 6438(1), F 54; 10. *Raistrickia rotunda* BAPal 6440(1), K49/3; 11. *Reticulatisporites passaspectus* BAPal 6440(1), S44/2; 12. *Tricidarisporites gutii* Césari and Limarino, 2002, BA Pal 6428(3), R55/1; 13. *Apiculatisporis variornatus* BAPal 6438(1), C29/4; 14. *Spelaeotriletes ybertii*, BAPal 6439(1), W20/1; 15. *Ahrensisporites cristatus* BAPal 6429(2), S44/4; 16. *Psomospora detecta*, BAPal 6430(1), X44/2; 17. *Cristatisporites menendezii* BAPal 6439(2), Y42/1; 18. *Plicatipollenites malabarensis* BAPal 6438(1), A43; 19. *Circumplicatipollis plicatus*, BAPal 6429(2), D38/3; 20. *Potonieisporites densus*, BAPal 6429(1), X52/4; 21. *Limitisporites* sp., BAPal 6429(2), G34/3 ; 22. *Potonieisporites brasiliensis*, BAPal 6432(1), F52/4; 23. *Striomonosaccites* sp. BAPal 6438(2), C29; 24. *Costatascyclus crenatus*, BAPal 6429(1), Q33/4; 25. *Caheniasaccites ovatus*, BAPal 6432(1), V53/1; 26. *Portalites gondwanensis*, BAPal 6438(1), G21/4; 27. *Tetraporina punctata*, BAPal 6446(1), Z49/1. Scale = 10 μm.

U–Pb zircon ages of 319.57 ± 0.09 Ma and 318.79 ± 0.10 Ma constrained the A Subzone of the DM Biozone to the late Serpukhovian–early Bashkirian (Césari et al., 2011).

The A Subzone can be compared with the oldest biozone of the palynostratigraphic scheme of the Brazilian Paraná Basin (Souza, 2006). The *Ahrensisporites cristatus* Biozone (Bashkirian–Kasimovian), related to the lowermost glacial levels of the Itararé Group, shares many species; however the Brazilian assemblages differ in the presence of uncommon (<5%) taeniate pollen. This compositional feature suggests a closer similarity with the Argentinian B Subzone and therefore a slight diachronism of the glacial event between the two regions.

A second issue raised in this paper refers to the time elapsed during the valley filling. In other words, was the valley quickly filled (some millions of years or less) or, on the contrary, was this glacial paleovalley

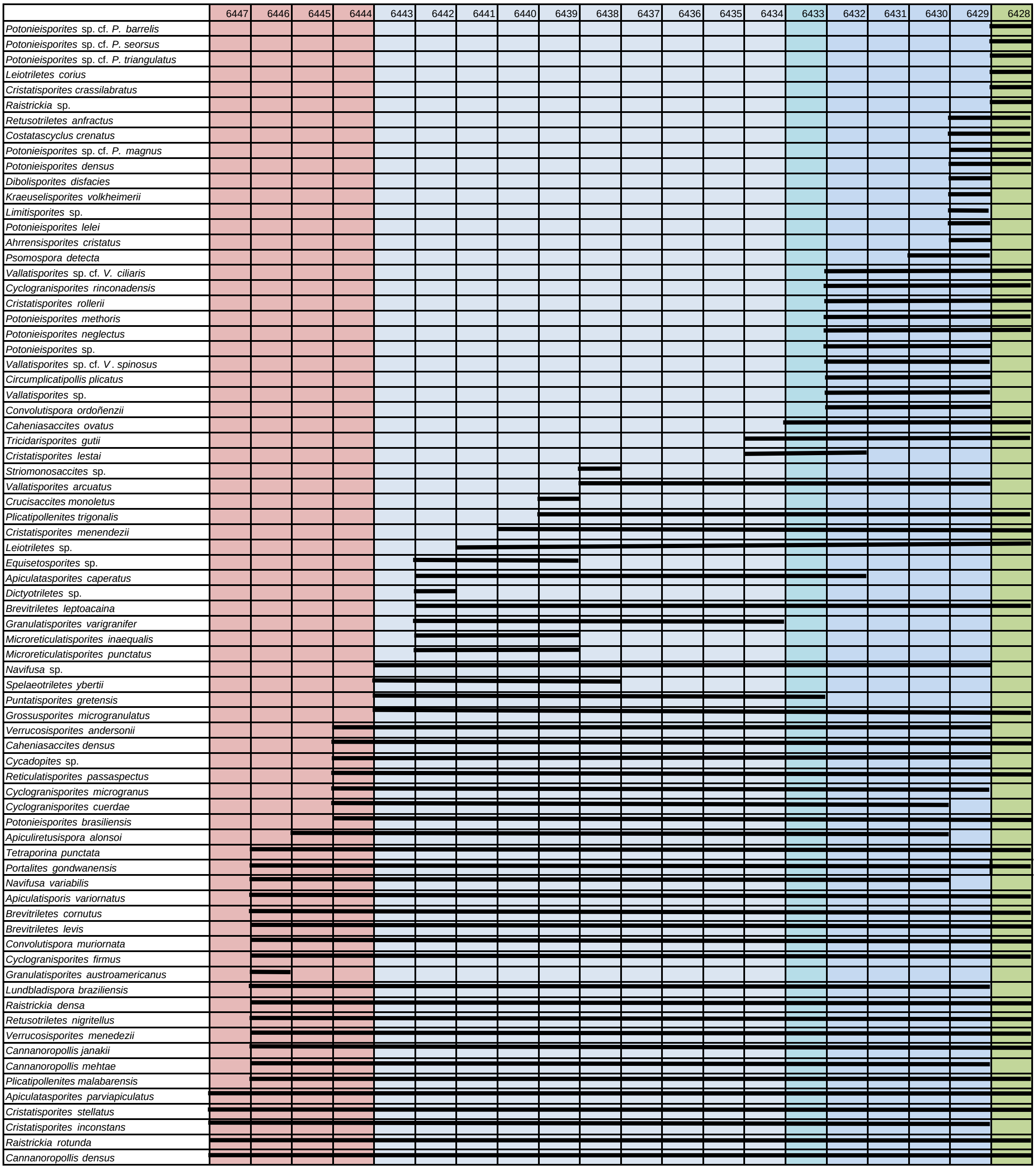

Fig. 12. Stratigraphic distribution of the palynological species.

worked through a long period of time (tens of millions of years)? The comparison of the palynological assemblages recovered from lower and upper sections does not seem to suggest a long time for the complete valley filling, indeed only assemblages belonging to the A Subzone of the DM Biozone were identified.

Fig. 13 proposes a model for the filling of the Veladero paleovalley in which the onset of the deglaciation corresponds to the lower section (Fig. 13A) characterized by the dominance of diamictite, lack of transgressive shale and high proportion of pollen grains. The progress of the deglaciation favored first the fluvial incision of the previously deposited diamictite, the subsequent flooding of the valley (onset of the fjord system, Fig. 13B) and then the progradation of Gylbert type deltas (Fig. 13C). The final stages of the fjord system are recorded in the fluvial conglomerate and sandstone included in the upper section (Fig. 13D).

Another interesting point concerns the variability in the palynomorphs within and between sections analyzed. The lower section shows the highest amount of pollen grains, a balanced pollen/spores ratio and absence of marine acritarchs (Fig. 13A). It is very likely that the postglacial marine flooding did not take place during the lower section and the sedimentation was restricted to small water bodies during the final retraction of the glaciers (Fig. 13A). The abundance of subaqueous stratified diamictite, and debris flow deposits, indicates reworking of previously deposited poorly sorted sediments probably linked to glacial geoforms (e.g. moraines). The frequent presence of dropstones shows that the glaciers were in contact with the water body. In this environment, the absence of marine palynomorphs reinforces the interpretation that the marine transgression had not yet flooded the valley. Moreover, the abundance of pollen grains and the

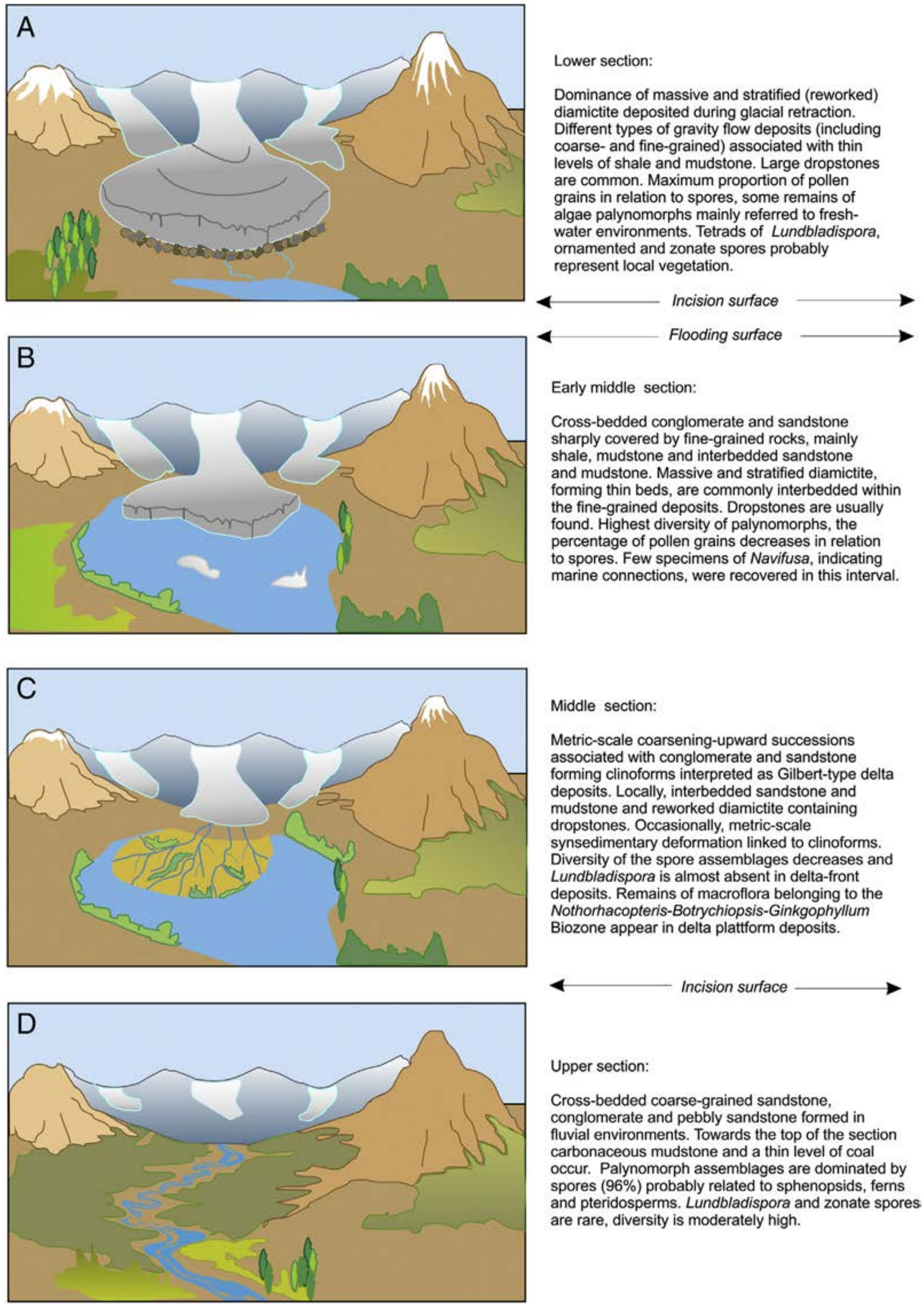

Fig. 13. Conceptual model for the evolution of sedimentary environments from the onset of the deglaciation (A) to the complete filling of the Veladero paleovalley (D).

balanced pollen/spore ratio suggest a plant-community composed by shrub-like vegetation in moist sites and forests of drier lands further upland.

The marine flooding of the valley is represented by the transgressive shale and prodelta fine-grained sediments that indicate the base of the middle section (Fig. 13B and C). It is precisely in this interval where scarce specimens of the marine *Navifusa* were found and where the percentage of pollen grains (linked to upland vegetation) begins to decrease, replaced by spores and algae related to plants growing around water bodies.

The shale and mudstone that mark the base of the transgression rest on an irregular incision surface carved into deposits belonging to the lower section. It is interesting to speculate on the origin of the high proportion of fragmentary pollen grains, which are commonly found in transgressive shale and prodelta deposits (base of the middle section). The reworking of pollen grains from the incised underlying lower section during the incision of fine-grained sediments should not be ruled out.

The low amount of marine palynomorphs and the lack of marine invertebrates have led to interpretations of similar deposits in the eastern

Paganzo Basin as proglacial and periglacial lakes (Limarino and Césari, 1988; Buatois et al., 1994). However, the discovery of marine invertebrates in some localities (Martínez, 1993), the presence of marine acritarchs related to the transgressive shale (Perez Loinaze et al., 2010a) and paleoenvironmental reconstructions (Limarino et al., 2002) allow for reinterpreting the transgressive shale as linked to a large postglacial marine transgression that flooded not only low-relief coastal regions (López Gamundí, 1987) but also paleovalleys forming fjord type environments (Dykstra et al., 2006; Limarino et al., 2010).

Finally, a new incision surface, although of low relief, was covered by conglomerate and sandstone deposited by braided fluvial systems. These deposits were succeeded by sandstone, mudstone and very scarce levels of coals that mark the complete filling of the valley (Fig. 13D).

Acknowledgments

We are grateful to Horacio Tassone for his help in the fieldtrips and processing of the palynological samples. We also thank Andrew M. Durbano (University of Saskatchewan) for his language review and two anonymous reviewers by their constructive comments. This research work was financed by projects PICT 1499 of the Agencia Nacional de Promoción Científica y Tecnológica and PIP 512 from the Conicet.

Appendix A. Palynomorph taxa listed in systematic order

SPORES

Ahrensisporites cristatus Playford and Powis 1979
Apiculatasporites caperatus Menéndez and Azcuy 1969
Apiculatasporites parviapiculatus Azcuy 1975
Apiculatisporis variornatus di Pasquo et al. 2003
Apiculiretusispora alonsoi Ottone 1989
Brevitriletes cornutus (Balme and Hennelly) Backhouse 1991
Brevitriletes leptoacaina Jones and Truswell 1992
Brevitriletes levis (Balme and Hennelly) Bharadwaj and Srivastava 1969
Convolutispora muriornata Menéndez 1965
Convolutispora ordonenzii Archangelsky and Gamerro 1979
Cristatisporites crassilabratus Archangelsky and Gamerro 1979
Cristatisporites inconstans Archangelsky and Gamerro 1979
Cristatisporites lestai Archangelsky and Gamerro 1979
Cristatisporites menendezii (Menéndez and Azcuy) Playford 1978
Cristatisporites rollerii Ottone 1989
Cristatisporites stellatus (Azcuy) Gutiérrez and Limarino 2001
Cyclogranisporites firmus Jones and Truswell 1992
Cyclogranisporites microgranus Bharadwaj 1962
Cyclogranisporites rinconadensis Césari and Limarino, 2002
Cyclogranisporites cuerdae Perez Loinaze et al. 2011
Dibolisporites disfacies Jones and Truswell 1992
Dictyotriletes sp.
Granulatisporites austroamericanus Archangelsky and Gamerro 1979
Granulatisporites varigranifer Menéndez and Azcuy 1971
Grossusporites microgranulatus (Menéndez and Azcuy) Perez Loinaze and Césari 2003
Kraeuselisporites volkheimerii Azcuy 1975
Leiotriletes corius Kar and Bose 1967
Leiotriletes sp.
Lundbladispora braziliensis (Pant and Srivastava) Marques-Toigo and Pons emend. Marques Toigo and Picarelli 1985
Microreticulatisporites inaequalis Menéndez and Azcuy 1973
Microreticulatisporites punctatus Knox 1950
Psomospora detecta Playford and Helby 1968
Punctatisporites gretensis Balme and Hennelly 1956
Raistrickia densa Menéndez 1965
Raistrickia rotunda Azcuy 1975
Raistrickia sp.
Reticulatisporites passaspectus Ottone 1991
Retusotriletes anfractus Menéndez and Azcuy 1969
Retusotriletes nigritellus (Luber) Foster 1979
Spelaeotriletes ybertii (Marques-Toigo) Playford and Powis 1979
Tricidarisporites gutii Césari and Limarino, 2002
Vallatisporites arcuatus (Marques-Toigo) Archangelsky and Gamerro 1979
Vallatisporites sp. cf. *V. ciliaris* Azcuy 1975
Vallatisporites sp. cf. *V. spinosus* Cauduro 1970
Vallatisporites sp.
Verrucosisporites andersonii (Anderson) Backhouse 1988
Verrucosisporites menendezii Archangelsky and Gamerro 1979

POLLEN GRAINS

Caheniasaccites densus Lele and Karim 1971 emend. Gutiérrez 1993
Caheniasaccites ovatus Bose and Kar emend. Gutiérrez 1993
Cannanoropollis densus (Lele) Bose y Maheshwari 1968
Cannanoropollis janakii Potonié y Sah 1960
Cannanoropollis mehtae (Lele) Bose y Maheshwari 1968
Circumplicatipollis plicatus Ottone y Azcuy 1988
Costatascyclus crenatus Felix y Burbridge emend. Urban 1971
Crusisaccites monoletus Maithy 1965
Cycadopites sp.
Equisetosporites sp.
Limitisporites sp.
Plicatipollenites malabarensis (Potonié and Sah) Foster 1975
Plicatipollenites trigonalis Lele 1964
Potonieisporites brasiliensis (Nahuys, Alpern and Ybert) Archangelsky and Gamerro 1979
Potonieisporites densus Maheshwari 1967
Potonieisporites lelei Maheshwari 1967
Potonieisporites methoris (Hart) Foster 1975
Potonieisporites neglectus Potonié and Lele 1961
Potonieisporites sp.
Potonieisporites sp. cf. *P. barrelis* Tiwari 1965
Potonieisporites sp. cf. *P. magnus* Lele and Karim 1971
Potonieisporites sp. cf. *P. seorsus* Playford and Dino 2000
Potonieisporites sp. cf. *P. triangulatus* Tiwari 1965
Striomonosaccites sp.

ALGAE

Navifusa variabilis Gutiérrez and Limarino 2001
Navifusa sp.
Tetraporina punctata (Tiwari and Navale) Kar and Bose 1976
Portalites gondwanensis Nahuys, Alpern and Ybert 1968

References

Aber, J.S., 1982. Model for glaciotectonism. Bull. Geol. Soc. Den. 30, 79–90.
Alonso-Muruaga, P.J., Limarino, C.O., Spalletti, L.A., Colombo Piñol, F., 2011. Findings of intraformational striated pavements in the Late Carboniferous glacial deposits of the Andean Precordillera, Argentina. Lat. Am. J. Sedimentol. Basin Anal. 18, 151–157.
Amy, L.A., Talling, P.J., Peakall, J., Wynn, R.B., Arzola Thynne, R.G., 2005. Bed geometry used to test recognition criteria of turbidites and (sandy) debrites. Sediment. Geol. 179, 163–174.
Archangelsky, S., Azcuy, C.L., González, C.R., Sabattini, N., 1987. Correlación general de biozonas. In: Archangelsky, S. (Ed.), El Sistema Carbonífero en la República Argentina. Academia Nacional de Ciencias, pp. 281–292.
Azcuy, C.L., Morelli, J.R., 1970. Geología de la comarca Paganzo-Amaná. El Grupo Paganzo. Formaciones que lo componen y sus relaciones. Rev. Asoc. Geol. Argent. 25, 405–429.
Balseiro, D., Rustán, J.J., Ezpeleta, M., Vaccari, N.E., 2009. A new Serpukhovian (Mississippian) fossil flora from western Argentina: paleoclimatic, paleobiogeographic and stratigraphic implications. Palaeogeogr. Palaeoclimatol. Palaeoecol. 280, 517–531.
Batten, D.J., 1996. Green and blue-green algae – Colonial chlorococcales. In: Jansonius, J., McGregor, D.C. (Eds.), Palynology: principles and applications. American Association of Stratigraphic Palynologist Foundation. 1, pp. 191–203.
Benn, D.I., Kirkbride, M.P., Owen, L.A., Brazier, V., 2005. Glaciated valley landsystems. In: Evans, D.J. (Ed.), Glacial Landsystems. Oxford University Press, pp. 372–406.
Bennett, M.R., Doyle, P., Mather, A.E., 1996. Dropstones: their origin and significance. Palaeogeogr. Palaeoclimatol. Palaeoecol. 121, 331–339.
Brugman, W.A., Eggink, J.W., Loboziak, S., Visscher, H., 1985. Late Carboniferous–Early Permian (Ghzelian–Artinskian) palynomorphs. J. Micropalaeontol. 4, 93–106.
Buatois, L.A., Limarino, C.O., Césari, S.N., 1994. Carboniferous lacustrine deposits from the Paganzo basin, Argentina. Global Geological Record of Lake Basins. 1, pp. 135–140.

Caputo, M.V., Melo, J.H.M., Streel, M., Isbell, J.L., 2008. Late Devonian and Early Carboniferous glacial records of South America. In: Fielding, C.R., Frank, T.D., Isbell, J.L. (Eds.), Resolving the Late Palaeozoic ice age in time and spaceGeological Society of America Special Paper. 441. The Geological Society of America, Inc., Tulsa, pp. 161–173.
Cazzulo-Klepzig, M., Menegat, R., Guerra-Sommer, M., 1995. Palynology and Palaeobotany in the reconstruction of landscape units from the Candiota Coalfield, Permian of Paraná Basin, Brazil. Rev. Bras. Paleontol. 8, 83–98.
Césari, S.N., Gutiérrez, P.R., 2001. Palynostratigraphy of Upper Paleozoic sequences in Central-Western Argentina. Palynology 24, 113–146.
Césari, S.N., Limarino, C.O., 2002. Palynology of glacial sediments from the Guandacol Formation (Middle Carboniferous) in the Cerro Bola area, Paganzo Basin, Argentina. Alcheringa 26, 159–176.
Césari, S.N., Limarino, C.O., Gulbranson, E., 2011. An Upper Paleozoic bio-chronostratigraphic scheme for the western margin of Gondwana. Earth Sci. Rev. 106 (1–2), 149–160.
Césari, S.N., Perez Loinaze, V.S., Limarino, C.O., 2013. La Biozona *Pakhapites fusus–Vittatina subsaccata* en la Formación Patquía (Pérmico), Precordillera de La Rioja, Argentina. 15. Revista Museo Argentino Ciencias Naturales n.s, pp. 71–88.
Clayton, G., 1995. Carboniferous miospore and pollen assemblages from the Kingdom of Saudi Arabia. Rev. Paleobotany Palynol. 89, 115–123.
Clayton, G., Loboziak, S., Streel, M., Turnau, E., Utting, J., 1990. Palynological events in the Mississippian (Lower Carboniferous) of Europe, North Africa and North America. Cour. Forsch. inst. Senckenb. 130, 79–84.
Combaz, A., Lange, F.W., Pansart, J., 1967. Les "Leiofusidae" Eisenack, 1938. Rev. Palaeobot. Palynol. 1, 207–307.
Cowan, E.A., Seramur, K.C., Cai, J., Powell, R.D., 1999. Cyclic sedimentation produced by fluctuations in meltwater discharge, tides and marine productivity in an Alaskan fjord. Sedimentology 46, 1109–1126.
Dallimore, A., Jmieff, D., 2010. Canadian west coast fjords and inlets of the NE Pacific Ocean as depositional archives. In: Howe, J.A., Austin, W.E.N., Forwick, M., Paetzel, M. (Eds.), Fjord Systems and Archives. Geological Society, London, Special Publications. 344, pp. 143–162.
De Blasio, F.B., Elverhøi, A., Engvik, L.E., Issler, D., Gauer, P., Harbitz, C., 2006. Understanding the high mobility of subaqueous debris flows. Nor. J. Geol. 86, 275–284.
Desjardins, P.R., Buatois, L.A., Limarino, C.O., Cisterna, G.A., 2009. Latest Carboniferous–earliest Permian transgressive deposits in the Paganzo Basin of western Argentina: lithofacies and sequence stratigraphy of a coastal-plain to bay succession. J. S. Am. Earth Sci. 28, 40–53.
Doublet, S., Garcia, J., 2004. The significance of dropstones in a tropical lacustrine setting, eastern Cameros Basin (Late Jurassic–Early Cretaceous, Spain). Sediment. Geol. 163, 293–309.
Dykstra, M., Kneller, B., Milana, J.P., 2006. Deglacial and postglacial sedimentary architecture in a deeply incised paleovalley-paleofjord; the late Carboniferous (Pennsylvanian) Jejenes Formation, San Juan, Argentina. Geol. Soc. Am. Bull. 118, 913–937.
Dykstra, M., Kneller, B., Milana, J.P., 2007. A high-resolution record of deep-water processes in a confined paleofjord, quebrada de Las Lajas, Argentina. In: Nilsen, T.H., Shew, R.D., Steffens, G.S., Studlick, J.R.J. (Eds.), Atlas of Deep-Water Outcrops: AAPG Studies in Geology. 56 (CD-ROM, 19 p.).
Eyles, N., Eyles, C.H., Miall, A.D., 1983. Lithofacies types and vertical profile models; an alternative approach to the description and environmental interpretation of glacial diamict and diamictite sequences. Sedimentology 30, 393–410.
Fielding, C.R., Frank, T.D., Isbell, J.L., 2008. The Late Paleozoic ice age—a review of current understanding and synthesis of global climate patterns. In: Fielding, C.R., Frank, T.D., Isbell, J.L. (Eds.), Resolving the Late Paleozoic Age in Time and Space. Geological Society of America Special Paper. 441, pp. 343–354.
González, C.R., 1981. Pavimento glaciario en el Carbónico de la Precordillera. Rev. Asoc. Geol. Argent. 36, 262–266.
González Bonorino, G., 1992. Carboniferous glaciation in northwest Gondwana continental margin. Evidence for grounded marine ice continental glaciation in southwestern Argentina. Palaeogeogr. Palaeoclimatol. Palaeoecol. 91, 363–378.
Gulbranson, E.L., Montañez, I.P., Schmitz, M.D., Limarino, C.O., Isbell, J.L., Marenssi, S.A., Crowley, J.L., 2010. High precision U–Pb calibration of Carboniferous glaciation and climate history, Paganzo Group, NW Argentina. Geol. Soc. Am. Bull. 122, 1480–1498.
Gustavson, T.C., Ashley, G.M., Boothroyd, J.C., 1975. Depositional sequences in glaciolacustrine deltas. In: Jopling, A.V., McDonald, B.C. (Eds.), Glaciofluvial and Glaciolacustrine Sedimentation. SEPM Special Publication. 23, pp. 264–280.
Hartshorn, J.H., 1958. Flowtill in southeastern Massachusetts. Bull. Geol. Soc. Am. 69, 477–482.
Henry, L.C., Isbell, J.L., Limarino, C.O., McHenry, L.J., Fraiser, M.L., 2010. Mid-Carboniferous deglaciation of the Protoprecordillera, Argentina recorded in the Agua de Jagüel palaeovalley. Palaeogeogr. Palaeoclimatol. Palaeoecol. 298, 112–129.
Huuse, M., Le Heron, D.P., Dixon, R., Redfern, J., Moscariello, A., Craig, J., 2012. Glaciogenic reservoirs and hydrocarbon systems: an introduction. Glaciogenic Reservoirs and Hydrocarbon Systems. Geological Society, London, Special Publications. 368, pp. 1–28.
Isbell, J.L., Miller, M.F., Wolfe, K.L., Lenaker, P.A., 2003. Timing of late Paleozoic glaciation in Gondwana: was glaciation responsible for the development of northern hemisphere cyclothems? In: Chan, M.A., Archer, A.W. (Eds.), Extreme Depositional Environments: Mega End Members in Geologic Time. Geological Society of America Special Paper. 370, pp. 5–24.
Kneller, B., Milana, J.P., Buckee, C., al Ja'aidi, O., 2004. A depositional record of deglaciation in a paleo-fjord (Late Carboniferous [Pennsylvanian] of San Juan Province, Argentina): the role of catastrophic sedimentation. Geol. Soc. Am. Bull. 116, 348–367.
Limarino, C.O., Césari, S.N., 1988. Paleoclimatic significance of the lacustrine Carboniferous deposits in northwest Argentina. Palaeogeogr. Palaeoclimatol. Palaeoecol. 65, 115–131.
Limarino, C.O., Césari, S.N., 1993. Reubicación estratigráfica de la Formación Cortaderas y definición del Grupo Angualasto (Carbonífero Inferior, Precordillera de San Juan). Rev. Asoc. Geol. Argent. 47, 61–72.
Limarino, C.O., Gutiérrez, P.R., 1990. Diamictites in the Agua Colorada Formation (northwestern Argentina): new evidence of Carboniferous glaciation in South America. J. S. Am. Earth Sci. 3, 9–20.
Limarino, C.O., Spalletti, L.A., 1986. Eolian Permian deposits in west and northwest Argentina. Sediment. Geol. 49, 109–127.
Limarino, C.O., Spalletti, L.A., 2006. Paleogeography of the Upper Paleozoic basins of Southern South America: an overview. J. S. Am. Earth Sci. 22, 134–155.
Limarino, C.O., Césari, S.N., Net, L.I., Marenssi, S.A., Gutiérrez, P.R., Tripaldi, A., 2002. The Upper Carboniferous postglacial transgression in the Paganzo and Río Blanco basins (northwestern Argentina): facies and stratigraphic significance. J. S. Am. Earth Sci. 15, 445–460.
Limarino, C., Tripaldi, S., Marenssi, S., Fauqué, L., 2006. Tectonic, sea-level, climatic controls on Late Paleozoic sedimentation in the western basins of Argentina. J. S. Am. Earth Sci. 22, 205–226.
Limarino, C.O., Spalletti, L.A., Colombo Piñol, F., 2010. Evolución paleoambiental de la transición glacial-postglacial en la Formación Agua Colorada (Grupo Paganzo), Carbonífero, Sierra de Narváez, NO argentino. Andean Geol. 37, 121–143.
Limarino, C.O., Césari, S.N., Spalletti, L.A., Taboada, A.C., Isbell, J.L., Geuna, S., Gulbranson, E.L., 2014. A paleoclimatic review of southern South America during the late Paleozoic: a record from icehouse to extreme greenhouse conditions. Gondwana Res. 25, 1396–1421.
Lindgren, S., 1980. Algal microfossils of the form genus *Tetraporina* from Upper Cretaceous clays, southern Sweden. Rev. Palaeobot. Palynol. 30, 333–359.
Loboziak, S., Clayton, G., 1988. The Carboniferous palynostratigraphy of northeast Libya. In: El–Arnauti, A., Owens, B. (Eds.), Subsurface Palynostratigraphy of Northeast Libya. Garyounis University, AGOCO/CIMP, Benghazi, pp. 129–149.
López Gamundí, O.R., 1984. Origen y Sedimentología de las diamictitas del Paleozoico Superior (con especial referencia a la cuenca Calingasta-Uspallata). Universidad de Buenos Aires, (Tesis Doctoral).
López Gamundí, O.R., 1987. Depositional models for the glaciomarine sequences of Andean Late Paleozoic basins of Argentina. Sediment. Geol. 52, 109–126.
López Gamundi, O.R., 1989. Postglacial transgressions in late Paleozoic basins of western Argentina: a record of glacioeustatic sea level rise. Palaeogeogr. Palaeoclimatol. Palaeoecol. 71, 257–270.
López Gamundí, O.R., 1997. Glacial-postglacial transition in the Late Paleozoic basins of southern South America. In: Martini, I.P. (Ed.), Late Glacial and Postglacial Environmental Changes-QuaternaryCarboniferous-Permian, and Proterozoic. Oxford, Oxford University Press, pp. 147–168.
López Gamundí, O.R., Martínez, M., 2000. Evidence of glacial abrasion in the Calingasta-Uspallata and western Paganzo basins, mid-Carboniferous of western Argentina. Palaeogeogr. Palaeoclimatol. Palaeoecol. 159, 145–165.
López Gamundí, O.R., Limarino, C.O., Césari, S.N., 1992. Late Paleozoic paleoclimatology of central west Argentina. Palaeogeogr. Palaeoclimatol. Palaeoecol. 91, 305–329.
Marenssi, S.A., Tripaldi, A., Limarino, C.O., Caselli, A.T., 2005. Facies and architecture of a carboniferous grounding-line system from the Guandacol Formation, Paganzo Basin, Northwestern Argentina. Gondwana Res. 8, 187–202.
Marr, J.G., Harff, P.A., Shanmugam, G., Parker, G., 2001. Experiments on subaqueous sandy gravity flows: the role of clay and water content in flow dynamics and depositional structures. Geol. Soc. Am. Bull. 113, 1377–1386.
Martínez, M., 1993. Hallazgo de fauna marina en la Formación Guandacol (Carbonífero) en la localidad de Agua Hedionda, San Juan, Precordillera Nororiental, Argentina. International Congress of Carboniferous–Permian. 2, pp. 291–296.
Melo, J.H.G., Loboziak, S., 2003. Devonian-Early Carboniferous miospore biostratigraphy of the Amazon Basin, Northern Brazil. Rev. Palaeobot. Palynol. 124, 131–202.
Miall, A.D., 1985a. Sedimentation on an early Proterozoic continental margin under glacial influence: the Gowganda Formation (Huronian), Elliot Lake area, Ontario, Canada. Sedimentology 32, 763–788.
Miall, A.D., 1985b. Architectural-element analysis: a new method of facies analysis applied to fluvial deposits. Earth Sci. Rev. 22, 261–308.
Miall, A.D., 1996. The geology of fluvial deposits. Sedimentary Facies, Basin Analysis, and Petroleum Geology, (582 pp.).
Milana, J.P., Bercowski, F., 1990. Facies y Geometría de depósitos glaciales en un paleovalle Carbonífero de Precordillera Central, San Juan, Argentina: 3ª Reunión Argentina de Sedimentología. Actas 199–204.
Mulder, T., Alexander, J., 2001. The physical character of subaqueous sedimentary density flows and their deposits. Sedimentology 48 (2), 269–299.
Mustard, P.S., Donaldson, J.A., 1987. Early Proterozoic ice-proximal glaciomarine deposition: the lower Gowganda Formation at Cobalt, Ontario, Canada. Geol. Soc. Am. Bull. 98, 373–387.
Ottone, E.G., Azcuy, C.L., 1989. Datos palinológicos de la Formación Guandacol (Carbonífero) en la quebrada de La Delfina, provincia de San Juan, Argentina. Ameghiniana 26, 191–208.
Perez Loinaze, V.S., Césari, S.N., 2012. Palynology of late Serpukhovian glacial and postglacial deposits from Paganzo Basin, northwestern Argentina. Micropaleontology 58, 335–350.
Perez Loinaze, V.S., Limarino, C.O., Césari, S.N., 2010a. Glacial events in Carboniferous sequences from Paganzo and Río Blanco Basins (northwest Argentina): palynology and depositional setting. Geol. Acta 8, 399–418.
Perez Loinaze, V.S., Limarino, C.O., Césari, S.N., 2010b. Palynological study of the Carboniferous sequence at Río Francia creek, Paganzo Basin, Argentina. Ameghiniana 48, 589–604.
Powell, R.D., 2005. Subaquatic landsystems: fjords. In: Evans, D.J. (Ed.), Glacial Landsystems. Oxford University Press, pp. 313–347.
Salfity, J.A., Gorustovich, S.A., 1983. Paleogeografía de la cuenca del Grupo Paganzo (Paleozoico Superior). Rev. Asoc. Geol. Argent. 38, 437–453.

Scalabrini Ortíz, J., 1973. El Carbónico en el sector septentrional de la Precordillera sanjuanina. Rev. Asoc. Geol. Argent. 27 (4), 371–373.
Scalabrini OrtÍz, J., Arrondo, O., 1973. Contribución al conocimiento del carbónico de los perfiles del Cerro Veladero y del Río del Peñón (Precordillera de La Rioja). Rev. Museo de La Plata (Nueva serie) 8 (68), 257–279.
Schomacker, E.R., Kjemperud, A.V., Nystuen, J.P., Jahren, J.S., 2010. Recognition and significance of sharp-based mouth-bar deposits in the Eocene Green River Formation, Uinta Basin, Utah. Sedimentology 57 (4), 1069–1087.
Shanmugam, G., 1996. High-density turbidity currents: are they sandy debris flows? J. Sediment. Res. 66, 2–10.
Souza, P.A., 2006. Late Carboniferous palynostratigraphy of the Itararé Subgroup, northeastern Paraná Basin, Brazil. Rev. Palaeobot. Palynol. 138, 1–29.
Spalletti, L.A., Limarino, C.O., Colombo Piñol, F., 2010. Internal anatomy of an erg sequence from the aeolian-fluvial system of the De La Cuesta Formation (Paganzo Basin, northwestern Argentina). Geol. Acta 8, 431–447.
Stoker, M.S., Wilson, C.R., Howe, J.A., Bradwell, T., Long, D., 2010. Paraglacial slope instability in Scottish fjords: examples from Little Loch Broom, NW Scotland. Fjord Systems and Archives. In: Howe, J.A., Austin, W.E.N., Forwick, M., Paetzel, M. (Eds.), Geological Society, London, Special Publications. 344, pp. 225–242.
Suárez-Soruco, R., 2000. Compendio de Geología de Bolivia. Rev. Técnica de Yacimientos Petrolíferos Fiscales Bolivianos 18, 1–144.
Taboada, A.C., 2010. Mississippian–Early Permian brachiopods from western Argentina: tools for middle- to high-latitude correlation, paleobiogeographic and paleoclimatic reconstruction. Palaeogeogr. Palaeoclimatol. Palaeoecol. 298, 152–173.
Tedesco, A.M., Limarino, C.O., Ciccioli, P.L., 2007. Primera edad radimétrica de los depósitos cretácicos de la Precordillera Central. Rev. Asoc. Geol. Argent. 62, 471–474.
Tedesco, A.M., Ciccioli, P.L., Suriano, J., Limarino, C.O., 2010. Changes in the architecture of fluvial deposits in the Paganzo Basin (Upper Paleozoic of San Juan province): an example of sea level and climatic controls on the development of coastal fluvial environments. Geol. Acta 8, 463–482.
Thomas, G.S., Connell, R.J., 1985. Iceberg drop, dump, and grounding structures from Pleistocene glacio-lacustrine sediments, Scotland. J. Sediment. Res. 55 (2).
Tiwari, R.S., Tripathi, A., Vijaya, 1995. Organic-walled microfossils of doubtful origin in Permian and Triassic sequences on peninsular India. Palaeobotanist 43, 1–38.
Van der Wateren, F.M., 1995. Structural geology and sedimentology of push moraines. Med. Rijks Geol. Dienst. 54, 1–168.
Varela, R., López de Luchi, M., Cingolani, C., Dalla Salda, L., 1996. Geocronología de gneises y granitoides de la sierra de Umango, La Rioja. Implicancias tectónicas. 13° Congreso Geológico Argentino y 3° Congreso de Exploración de Hidrocarburos. Actas, pp. 519–527 (Buenos Aires).
Varela, R., Sato, A.M., Basei, M., Siga, O., 2003. Proterozoico medio y Paleozoico inferior de la sierra de Umango, antepais andino (29°S). Argentina: edades UPb y caracterizaciones isotópicasRevista de la Asociación geológica de Chile. 30. Servicio Nacional de Geología y Minería, Santiago de Chile, pp. 265–284.
Zhu, H., 1993. A revised palynological sub–division of the Namurian of Jingyuan, northwest China. Rev. Palaeobot. Palynol. 77, 273–300.
Zielinski, T., van Loon, A.J., 1996. Characteristics and genesis of moraine-derived flowtill varieties. Sediment. Geol. 101, 119–143.
Zippi, P.A., 1998. Freshwater algae from the Mattagami Formation (Albian, Ontario), palaeoecology, botany and systematic taxonomy. Micropaleontology 44, 98–103.